AD-A139 800 ENVIRONMENTAL SUPPORT FOR PROJECT WEAP (WEAPONS ENVIRONMENTAL ACOUSTIC PR..(U) NAVAL OCEAN RESEARCH AND DEVELOPMENT ACTIVITY NSTL STATION MS.. 1/1

UNCLASSIFIED M D RICHARDSON ET AL. OCT 83 NORDA-40 F/G 8/10 NL

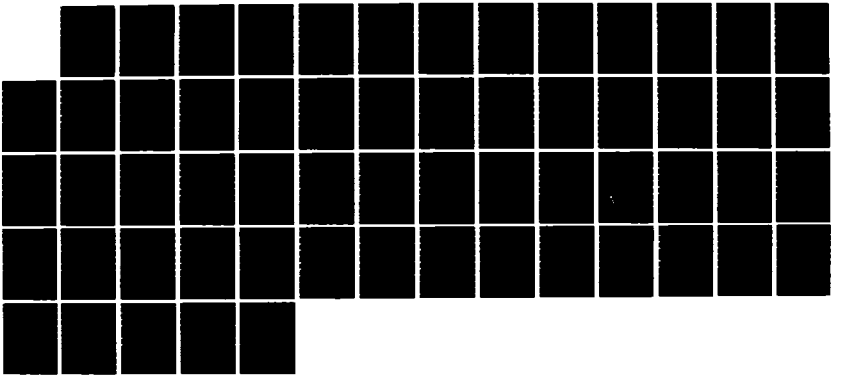

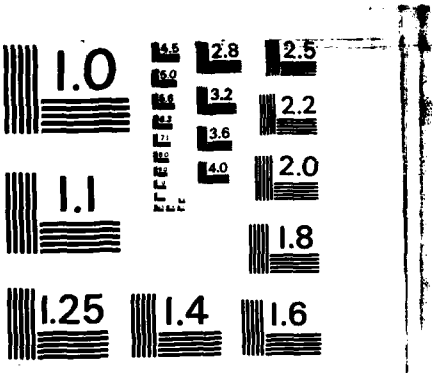

NORDA Report 40

Environmental Support for Project WEAP East of Montauk Point, New York 7-28 May 1982

Michael D. Richardson
John H. Tietjen*
Richard I. Ray

Oceanography Division
Ocean Science Directorate

October 1983

*City College of New York
Department of Biology
New York, N.Y. 10031

Naval Ocean Research and Development Activity
NSTL, Mississippi 39529

Foreword

High resolution acoustic and environmental data are required for new concepts in the design of weapon systems. These design concepts require the statistical variability of acoustic and environmental data in order to model the effects of ocean bottom and surface boundaries on transmitted acoustic signals.

This report presents the biological and geoacoustic data required to model forward, back, and out-of-plane scattering from the sediment-water interface, collected for Project WEAP a joint Naval Ocean Research and Development Activity/Naval Underwater Systems Center high frequency acoustic experiment.

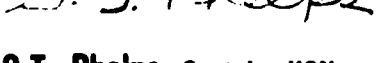

G.T. Phelps, Captain, USN
Commanding Officer, NORDA

Executive Summary

This report covers environmental support for Project WEAP (Weapons Environmental Acoustics Program), a joint Naval Underwater Systems Center (NUSC), Naval Ocean Research and Development Activity (NORDA) high frequency acoustic experiment, conducted 25 km east of Montauk Point, Long Island, New York. The objective of Project WEAP was to provide the high resolution acoustic and environmental data required for new concepts in weapon system design.

The acoustic experiment was sited at the southern terminus of a drowned barrier spit in 35 m of water. Sediment and faunal samples were collected remotely with a 0.025 m^2 box core. Scuba diver collected sediment cores were obtained to measure sediment geoacoustic properties.

Two sediment types (fine sand and coarse sand) were evident from the laboratory analysis of sediment grain size. Fine sand sediments had lower values of compressional wave velocity, impedance, and bulk density; lower reflection coefficients and higher bottom loss and attenuation values than coarse sand sediments.

Geoacoustic Property	Sediment Type	
	Fine Sand	Coarse Sand
Mean Grain Size (Ø)	2.07	0.00
Porosity (%)	36.5	--
Sediment Density (g/cm^3)	2.05	2.37
Compressional Wave Velocity (m/sec) @ 6°C, 32.4 ppt, 36 m	1677	1728
Attenuation (k)	0.22	0.17
Sediment Impedance ($g/cm^2 sec$ 10^5) @ 6°C, 32.4 ppt, 36 m	3.41	4.10
Rayleigh Reflection Coefficient	0.39	0.46
Bottom Loss (dB) @ normal incidence	8.3	6.7

Measured compressional wave velocity values were 3 to 5 percent lower than the values derived from empirical predictor equations for fine sand sediments, while attenuation values were one-half predicted

Executive Summary, (continued)

values. We estimate that predicted compressional wave velocity for coarse sand was 8 percent higher than actual values. We, therefore, calculated sediment acoustic properties for coarse sand sediments based on compressional wave velocity of 1728 m/sec instead of the empirically predicted 1878 m/sec. This yielded lower than predicted (from mean grain size) sediment impedance and reflection coefficients and higher bottom loss. Estimated attenuation values were also lower than those empirically predicted.

The within core and within station variability of sediment geoacoustic properties was low, partially a result of sediment mixing by benthic invertebrates. The areal (between station) variability in sediment geoacoustic properties was high because present hydrodynamic and historical geological processes created a two sediment system: a light-colored, well-sorted, fine sand discontinuously covered a reddish, coarse, granular sediment.

The fine sand was similar to most sediments found on the middle Atlantic Sand Plain. This sediment was derived from weathering products transported from adjacent land during previous glacial regressions. The reddish coarse sand was a lag deposit formed from the erosion of the drowned barrier spit. The fine sand was in dynamic equilibrium with severe storms which occur in this area while the coarse sand was in equilibrium with rarer, very severe storms. The areal distribution of these sediment types was not predictable from historical data and probably changes with season and severe storm events. Side scan sonar imagery techniques are required to delineate the distribution of both sediment types. Had the experiment been sited 10 m deeper sediment geoacoustic properties and microtopography could have been more precisely predicted, because of less heterogeneity in sediments.

The distribution of faunal assemblages paralleled the distribution of sediment types. The fine sand substrate (Stations 3, 4, 5, 7, 8, 9, and 10) was dominated by tube-building ampeliscid amphipods, free-burrowing haustoriid amphipods, and the sand dollar, Echinarachnius parma. Amphipods contributed 55 percent of the faunal density at these stations while

sand dollars accounted for 79 percent of the biomass. The coarse sand substrate (Stations 6, 11, 12, and 13) was dominanted by the errant polychaetes Drilonereis magna, Drilonereis longa, Goniada maculata and Glycera capitata. Also abundant was the tube-dwelling polychaete Clymenella torquata.

Bioturbation by the sand dollar, Echinarachnius parma, mixed the upper few centimeters of sediment, changing sediment geoacoustic properties and modifying and distroying microtopography. E. parma probably contributes to bottom forward and backscatter at 40 and 80 kHz where their calcareous bodies act as point surface scatterers, and at all frequencies where sand dollars overlap. The sediment microtopography created by E. parma probably contributes to resonance scattering of all frequencies used in Project WEAP (5 to 80 kHz).

It is estimated that, the tube dwelling polychaete Clymenella torquata turns over the upper 20 cm of sediment at one station in 0.42 yr. This activity may create considerable microtopography and sediment volume heterogenity in geoacoustic properties, which probably contributes to resonance and volume scattering at the coarse sand stations.

Recommendations for future shallow-water acoustic experiments are given. Collection of in-situ environmental data is suggested. The use of extensive presite surveys is strongly urged in order to site the experiment in a homogeneous area or at least in an area where heterogeneities can be predicted and mapped. Detailed methodologies and philosophies for environmental sampling are given. These approaches should yield the physical and empirical submodels required to extrapolate acoustic bottom reverberation prediction beyond the measured data.

Acknowledgments

The authors particularly thank William Roderick and his coworkers at the Naval Underwater Systems Center for logistics support. We also thank David K. Young and Steve Stanic, both of NORDA, for their careful review of this manuscript. William Roderick and Jim Sycks of NUSC provided the underwater photographs used in this report. Roxanne Mauffray typed the manuscript. This work was supported by NAVSEA Program Element 62759N, Edward D. Chaika (FY82) and Robert L. Martin (FY83) Program Managers.

Contents

Contents, (continued)

Illustrations

Illustrations, (continued)

Tables

Tables, (continued)

Environmental Support for Project WEAP East of Montauk Point, New York, 7-28 May 1982

Part A: Sediment Acoustic and Physical Properties

Michael D. Richardson, Richard L. Ray

I. Introduction

This report covers environmental support for a joint Naval Underwater Systems Center (NUSC), Naval Ocean Research and Development Activity (NORDA) high frequency acoustic experiment. The experiment was conducted 25 km east of Montauk Point, Long Island, New York (41°04'N, 71°35'W) in a water depth of 35 m.

The objective of Project WEAP (Weapons Environmental Acoustics Program) was to provide the high resolution acoustic and environmental data required for new concepts in the design of weapon systems. These design concepts require the statistical variability of acoustic and environmental data in order to model the effects of ocean bottom and surface boundaries on transmitted acoustic signals.

In this report we provide the biological and geoacoustic data required to model forward, back and out-of-plane scattering from the sediment-water interface. Acoustic scattering and bottom roughness data will be reported elsewhere.

The combined environmental and acoustic data will not only be important for weapon systems design and performance prediction but invaluable for acoustic submodel development and verification (Stanic et al., 1983). Most of the empirical predictive submodels used today are based on limited data sets, have not been validated, or do not cover the acoustic and environmental conditions of interest to weapon system developers. It is hoped that this project will provide the high quality environmental data required to solve some of these problems.

II. Materials and Methods

A. Description of Study Site

Experiments were conducted at a site 25 km east of Montauk Point, Long Island, New York (41°04'N, 71°35'W) (Fig. 1). This site was chosen for logistic and environmental reasons. The presumed bottom type, a gray-white sand with current controlled sand waves (McMaster and Garrison, 1967), was considered a good reflector and scatterer of acoustic energy. During May, the sound speed gradient would be slightly negative causing downward refraction propagation conditions, an obvious requirement for bottom scattering experiments (Roderick, 1982). The water depth, 35 m, was within the operational limits of scuba divers, who took stereophotographs for bottom roughness determination. The site was also a short transit from port for the research vessels, USNS LYNCH and R/V SHOCK, involved in the experiment.

Bathymetry, morphology and surficial sediment properties of the middle Atlantic Bight have been summarized by Duane et al. (1972), Swift et al., (1972, 1973), Schlee (1973), and Freeland and Swift (1978).

The inner continental shelf topography is dominated by a ridge and swale topography. Ridges off Long Island are about 2 km apart and have 2-10 m amplitudes. These features, once thought to be relicts of barrier island and beach dune topography, are now considered to be in dynamic equilibrium with present hydrographic conditions (Duane et al., 1972 and Swift et al., 1973).

The study site is part of the drowned barrier spit-lagoon-headland complex

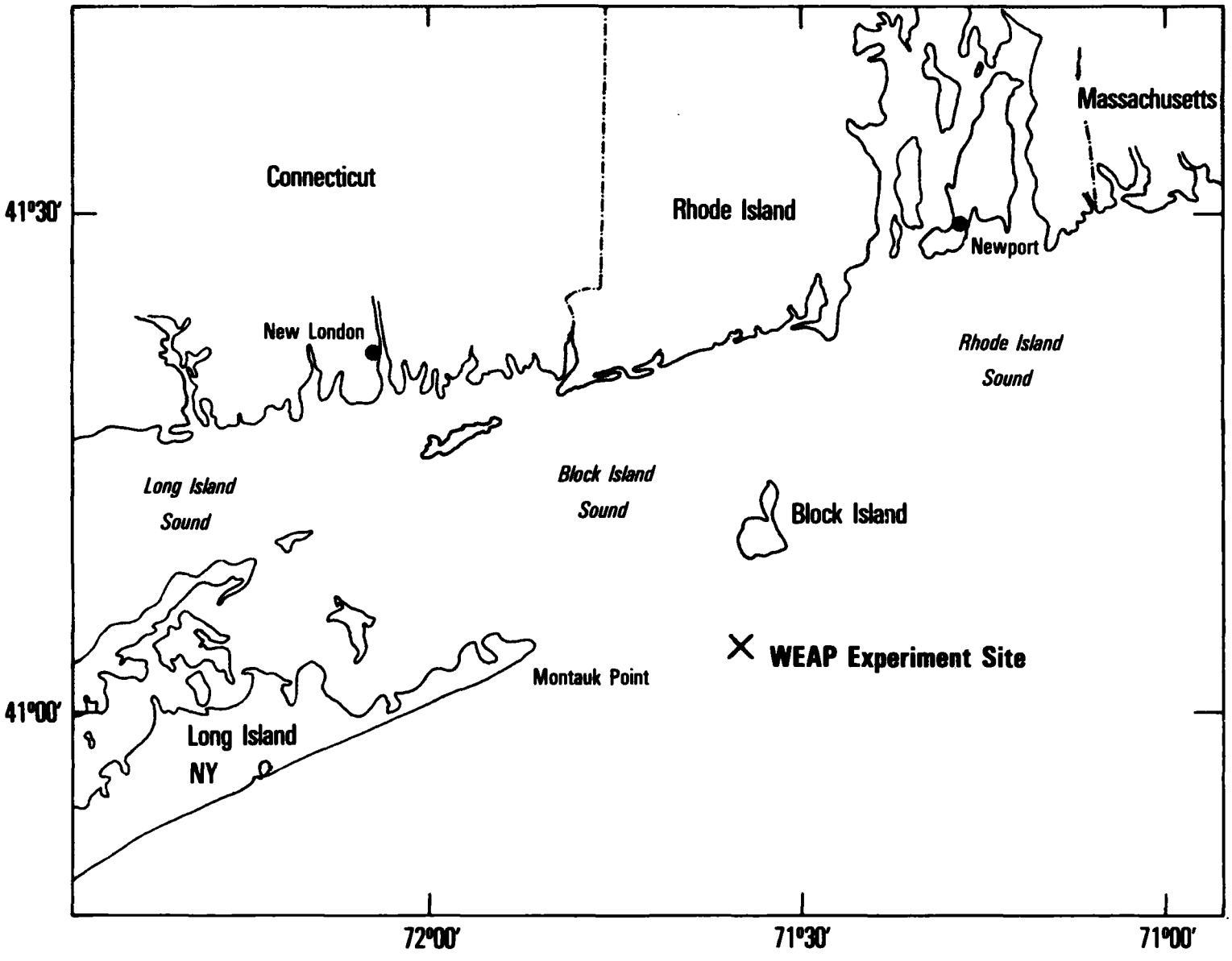

Figure 1. Location of experimental site

described by McMaster and Garrison (1967) (Fig. 2). This feature was preserved because this particular barrier spit was tied to a rocky peninsula of glacial debris (Swift et al., 1972). The acoustic experiment was sited at the southern terminus of the drowned spit in a water depth of 35 m. Sediments that formed the spit were probably eroded glacial material from the rocky headland.

Visual observations from a submersible were made of the spit by McMaster and Garrison (1967) (Fig. 2, transect Z). Sediments graded from boulder size particles at 23 m to a poorly sorted mixture of sand and gravel at 27 m. Below 27 m poorly sorted sediment was gradually replaced by a reddish, well-sorted, granular sediment. This reddish sediment was covered by a light-colored, well-sorted fine sand below 33 m. The light-colored fine sand was characterized by small, irregular discontinuous ripple marks which migrated under the influence of tidal currents while the reddish granular sediments were characterized by

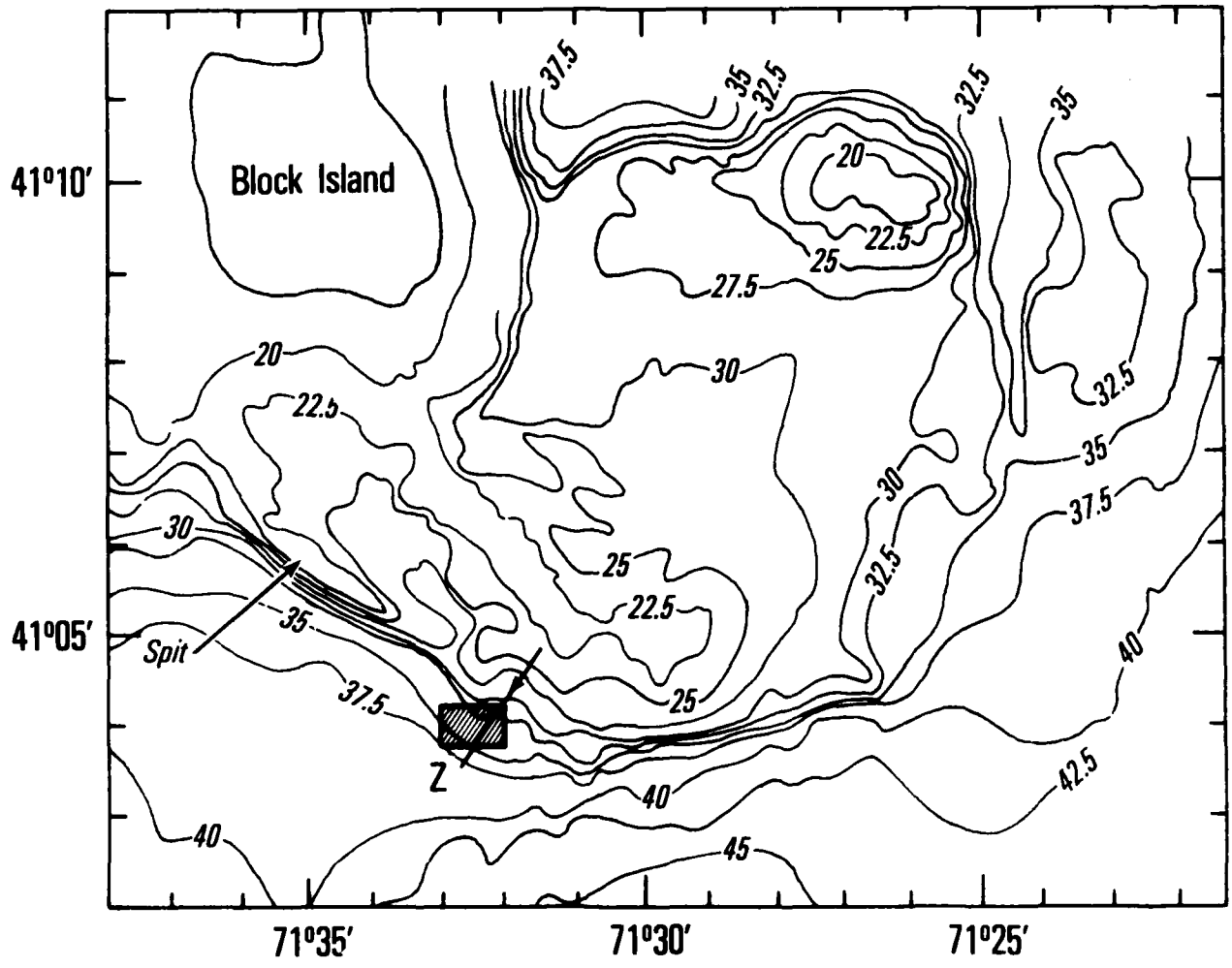

Figure 2. Bottom topography near the experimental site showing the drowned barrier spit-lagoon-headland complex. Cross hatched area represents the experimental site.

larger (75 cm period, 15-20 cm amplitude) symmetrical ripples.

B. Field Collection

A plan view of the experimental site with locations of sediment samples, the parametric projector-receiver, and the hydrophone receiving array is presented in Figure 3. Samples were collected either remotely with a 0.025 m^2 box core or directly by scuba divers (Table 1).

Subsamples consisting of either 10 g of sediment from the surface or cylindrical sediment cores were collected from retrieved box cores (Stations 1-13). These samples were used to determine the areal and vertical distribution of sediment grain size. Cylindrical acrylic cores were used by scuba divers to collect sediment at a location midway between parametric projector and hydrophone receiving array (Station 14). These samples were used to determine sediment acoustic and physical properties near the infection point for comparison with acoustic forward scattering data.

All cylindrical cores were 45 cm long, had a 6.1 cm inside diameter, and were bevelled at one end to improve penetration into the sediment. Diver-collected cores were capped at both ends immediately after collection to retain overlying water and kept in an upright position during transport. We were unable

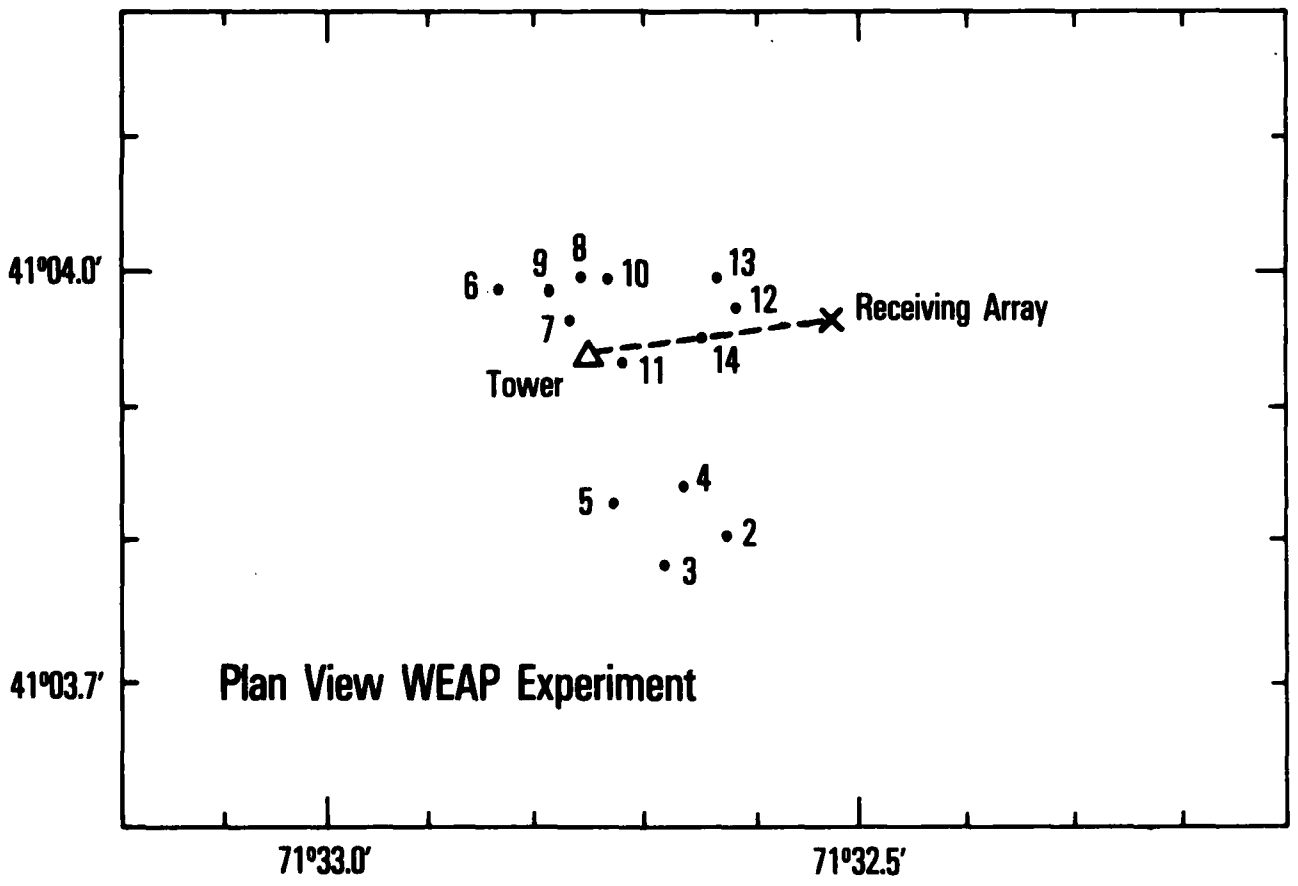

Figure 3. Plan view of experimental site showing the location of the parametric projector-receiver, hydrophone receiving array and thirteen sampling sites.

Table 1. Summary of sample locations

Station	Latitude	Longitude	Depth (m)
1	41°05.29'	71°32.99'	41.1
2	41°03.81'	71°32.63'	36.3
3	41°03.79'	71°32.69'	36.6
4	41°03.85'	71°32.67'	36.3
5	41°03.84'	71°32.73'	36.5*
6	41°03.99'	71°32.84'	36.6
7	41°03.97'	71°32.77'	35.4
8	41°04.00'	71°32.76'	35.4
9	41°03.99'	71°32.79'	36.0*
10	41°04.00'	71°32.74'	34.4
11	41°03.94'	71°32.72'	35.0*
12	41°03.98'	71°32.62'	35.0*
13	41°04.00'	71°32.64'	35.0*
14	41°03.95'	71°32.65'	35.0*

* Estimated depths

to retain water overlying the sediment in the box core samples because of the poor sealing characteristics of the box core in these coarse grained sands. Acoustic measurements were, therefore, not made on box core samples.

Acoustic measurements on cores collected at Station 14 were made at sea within 12 hours of collection. All sediment samples were then transported on ice to laboratory facilities at NSTL for physical property analysis.

C. Laboratory Analysis

Sediment temperature was equilibrated to room temperature prior to acoustic measurements. Temperature and salinity of the overlying water were measured with a YSI Model 43TD temperature probe and an AO Goldberg temperature-compensated, salinity refractometer.

Values of sediment compressional wave velocity and attenuation were determined at 1 cm intervals in the core samples with an Underwater System, Inc. (Model USI-103) transducer-receiver head. A Tektronic PG 501 Pulse Generator and FG 504 Function Generator, Krohn-Hitz 3100R Band Pass Filter and a Hewlett-Packard 1743A dual-time interval oscilloscope were substituted for the electronics unit and oscilloscope usually employed with the USI-103 Velocimeter (Fig. 4). These substitutions increased resolution of compressional wave velocity measurements and provided accurate measurement of received voltages required for attenuation measurements.

The transducer was driven with a 400 kHz, 20 volt p-p sine wave triggered for 25μ duration every 2 msec using the pulse generator and function generator. The received signal was filtered (1-1000 kHz high cut-off and low cut-off) prior to making time delay and received voltage measurements. Time delay measurements were made at the fourth sine wave zero crossing. Received voltage measurements were made utilizing the maximum peak height of the fourth sine wave.

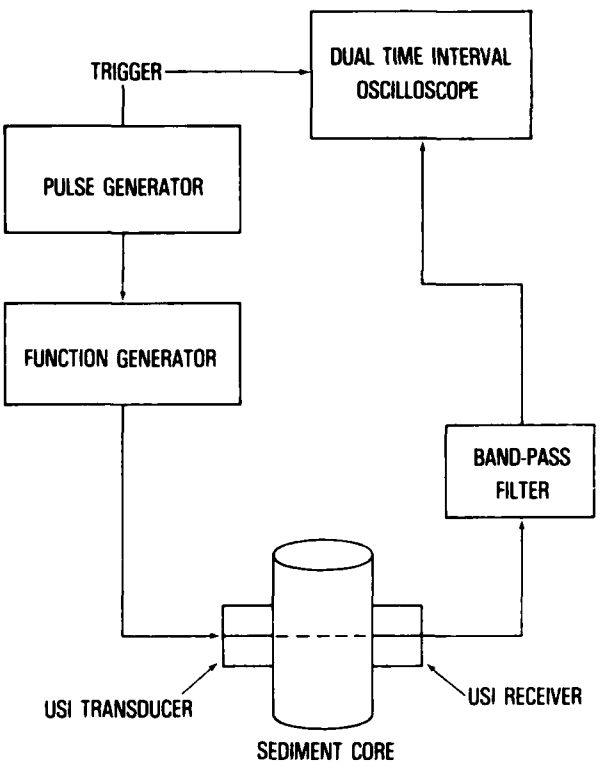

Figure 4. Block diagram of compressional wave velocity and attenuation measuring system

Sediment compressional wave velocity was determined by comparison of similar time delay measurements made on the overlying salt water and sediments using the following formula:

$$V = \frac{C(w)}{1 - \frac{\Delta t C(w)}{d}} \quad (1)$$

where V is the sound velocity through sediment (m/sec); C(w) is the sound velocity through salt water (m/sec); Δt is the measured time arrival through sediment (sec); and d is the inside diameter of the core (m). All sound velocities were calculated at the temperature, salinity and pressure (23°C, 35 ppt, 1 atm) suggested by Hamilton (1971) and the approximate in situ conditions at the time of the experiment (6°C, 32.4 ppt, 35 m).

Attenuation measurements were calculated as 20 log of the ratio of the received voltage through salt water versus received voltage through sediment. Attenuation measurements were extrapolated to a 1 m path length and reported as dB/m (Hamilton, 1972). Attenuation was also expressed as a sediment specific constant (k):

$$\alpha = kf^n \quad (2)$$

where α is the attenuation of compression waves in sediment (dB/m), f is the transmitted signal frequency (kHz) and n is a measure of frequency dependence. If n is assumed to be 1 (Hamilton, 1972), then the sediment specific constant (k) can be used to compare sediment attenuation to other sediment physical properties such as porosity and mean grain size without regard to the frequency at which the measurements were made.

After acoustic measurements were made, sediment from the three replicate cores from Station 14 and from Stations 2, 3, 4, 5, and 11 were extruded and sectioned at 2 cm intervals for grain size analysis. Sediment grain size distribution was determined for all sediment samples with an ATM Sonic Sifter for gravel and sand sized particles and by the pipette method for percent silt and percent clay. Mean phi, standard deviation, kurtosis, and normalized kurtosis were calculated according to the graphic formula of Folk and Ward (1957). Porosity was determined as weight loss of sediment dried at 105°C for 24 hours.

III. Results

A. Sediment Physical Properties

Two sediment types were evident from the laboratory analysis of grain size (Appendix A). Stations 3, 4, 5, 7, 8, 9, 10, and 14 were characterized by moderately well-sorted, near symmetrical to coarse-skewed fine sand. Stations 2, 6, and 11 were characterized by poorly sorted, near symmetrical to fine skewed, coarse to very coarse sand. Stations 12 and 13 contained poorly sorted, near symmetrical coarse to very coarse sands which apparently contained a mixture of the other two sediment types.

Sediments collected from the fine sand substrate had a nearly uniform distribution of sediment grain size properties throughout the length of each core. Sediments collected from the coarse sand substrate (Stations 2 and 11) had greater downcore variability in grain size properties. Mean grain size, a predictor of sediment acoustic properties, followed the same trends as the dominant phi modes (Fig. 5).

Porosity values ranged from 34.5 to 38.2% for sediment collected by scuba divers from Station 14 (Fig. 6). Surface porosity value of 41.1% from core 14-2 probably resulted from inclusion of the overlying water in the 0-2 cm sediment fraction. Porosity values decreased 3% with depth in core 14-2 but remained constant in core 14-1.

B. Sediment Acoustic Properties

Sediment compressional wave velocity (m/sec); velocity ratio; and attenuation

(α) expressed as dB/m @ 400 kHz, and k were calculated at 1 cm intervals for the three cores collected from Station 14 (Table 2). Compressional wave velocity was calculated for the approximate in-situ conditions of 6°C, 32.4 ppt salinity and 36 m water depth.

We found no significant difference in the mean values of velocity or attenuation between the three cores collected at Station 14 (Table 2). A slight increase in compressional wave velocity with depth in cores of 10 to 20 m/sec was noted (Fig. 7). Compressional wave attenuation was too variable for down-core trends to be evident (Fig. 8).

IV. Discussion

A. *Variability of Sediment Geoacoustic Properties*

It has been shown that sediment geoacoustic properties such as compressional wave velocity, sediment mean grain size, and sediment porosity can be quite variable in shallow coastal marine sediments (Richardson et al., 1983a, b). The within core variability (Table 3) of sediment geoacoustic properties from this experiment was about the same as for samples collected from sandy sediments one mile off Mission Beach, California, (Richardson et al., 1983b) but much lower than for silty-clay sediments from Long Island Sound (Richardson et al., 1983a).

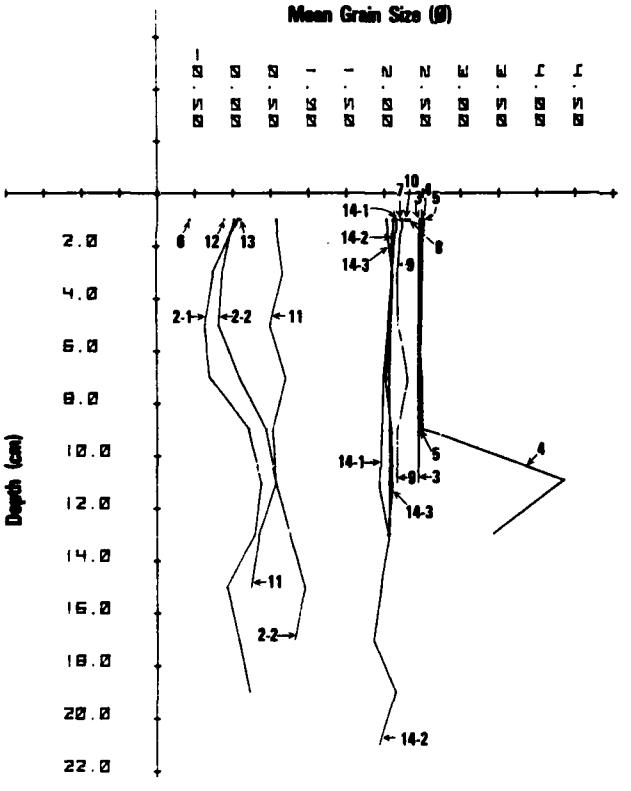

Figure 5. Vertical distribution of sediment mean grain size (Ø) for cores collected at Stations 2, 3, 4, 5, 9, 11 and 14 and mean grain size for surface samples collected at Stations 6, 7, 8, 10, 12 and 13

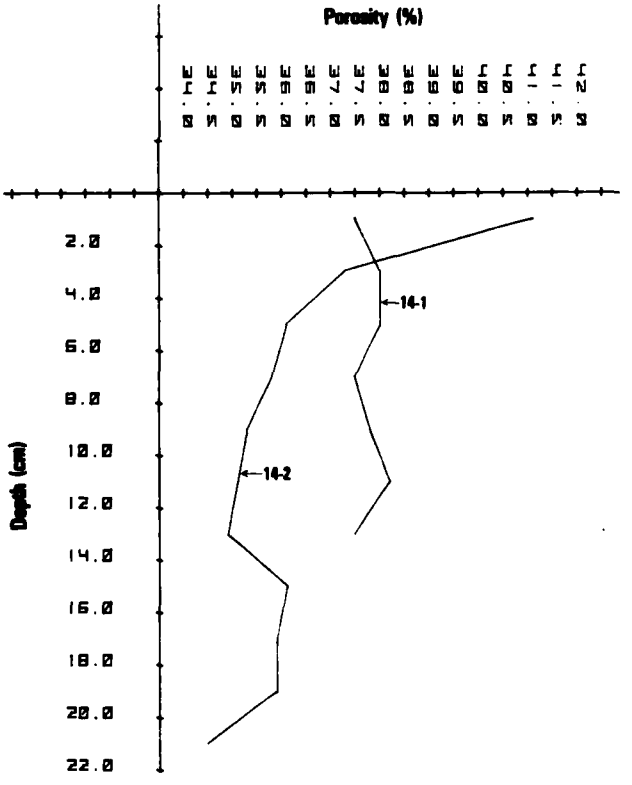

Figure 6. Vertical distribution of porosity (%) for two cores collected at Station 14

Table 2. Values of compressional wave velocity, velocity ratio, and attenuation measured from three cores collected at Station 14

Depth (cm)	V_p	V_p Ratio	α	k
Station 14-1				
1.0	1649.3	1.120	125.3	0.313
2.0	1663.3	1.130	81.8	0.205
3.0	1667.1	1.133	78.1	0.195
4.0	1668.0	1.133	83.7	0.209
5.0	1673.7	1.137	93.5	0.234
6.0	1668.5	1.134	125.3	0.313
7.0	1677.6	1.140	115.5	0.289
8.0	1684.3	1.144	89.5	0.224
9.0	1684.8	1.145	85.6	0.214
10.0	1687.7	1.147	81.8	0.205
11.0	1683.3	1.144	106.3	0.266
Station 14-2				
1.0	1637.3	1.112	205.0	0.512
2.0	1651.6	1.122	101.9	0.255
3.0	1660.9	1.128	89.5	0.224
4.0	1664.2	1.131	85.6	0.214
5.0	1671.3	1.135	89.5	0.224
6.0	1669.4	1.134	74.5	0.186
7.0	1680.9	1.142	81.8	0.205
8.0	1682.9	1.143	74.5	0.186
9.0	1686.2	1.146	74.5	0.186
10.0	1692.6	1.150	83.7	0.209
11.0	1690.6	1.149	104.1	0.260
12.0	1683.8	1.144	93.5	0.234
13.0	1676.6	1.139	93.5	0.234
14.0	1679.0	1.141	93.5	0.234
15.0	1682.9	1.143	83.7	0.209
16.0	1691.1	1.149	93.5	0.234
17.0	1691.1	1.149	93.5	0.234
18.0	1691.1	1.149	115.5	0.289
Station 14-3				
1.0	1643.7	1.117	100.9	0.252
2.0	1646.0	1.118	88.1	0.220
3.0	1648.3	1.120	92.3	0.231
4.0	1644.2	1.117	88.1	0.220
5.0	1640.0	1.114	69.1	0.173
6.0	1647.4	1.119	78.3	0.196
7.0	1656.2	1.125	69.1	0.173
8.0	1657.7	1.126	69.1	0.173
9.0	1657.7	1.126	69.1	0.173
10.0	1654.8	1.124	69.1	0.173

Within station variability of sediment geoacoustic properties for Station 14 was not significantly greater than for individual cores. Areal (between station) variability in mean grain size was considerable. Mean grain size values for the upper 2 cm of sediment ranged from -0.57 Ø at Station 6 to 2.51 Ø at Station 5. These differences were related to the biological processes, hydrodynamic processes, and historical causes discussed in Part C.

B. *Prediction of In-situ Sediment Impedance, Attenuation and Bottom Loss at Normal Incidence*

Sediment physical properties such as porosity and mean grain size can be used to calculate sediment impedance and bottom loss (Table 4). These values are required as inputs for submodels which

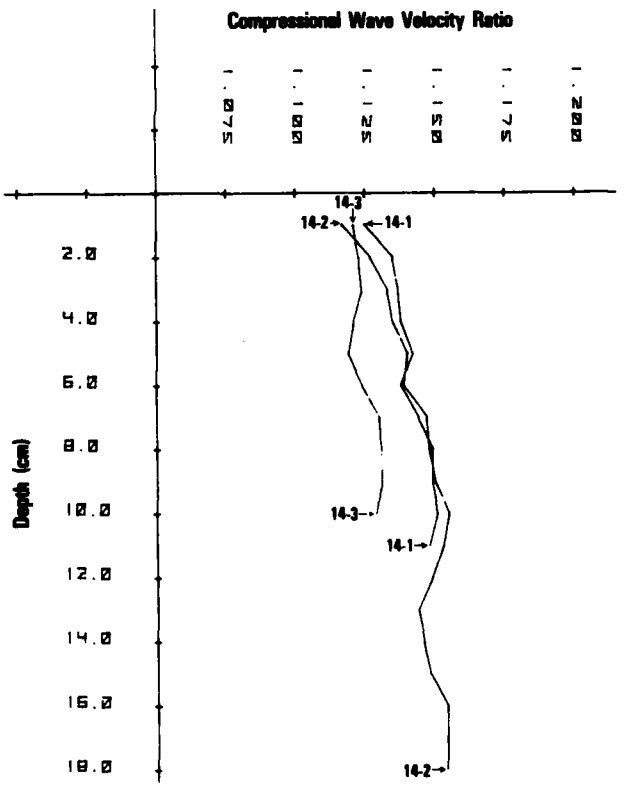

Figure 7. Vertical distribution of compressional wave velocity ratio for three cores collected at Station 14

predict acoustic backscatter at the sediment-water interface.

Sediment bulk density, ρ (g/cm^3), was predicted from mean grain size (M_z) using equation (3) from Hamilton and Bachman (1982)

$$\rho = 2.374 - 0.175M_z + 0.008M^2_z. \quad (3)$$

Where possible sediment bulk density was also directly calculated from porosity assuming a grain density of 2.65 g/cm^3 (quartz) and an interstitial water density of 1.0255 g/cm^3. Compressional wave velocity was predicted from mean grain size using the following equation from Hamilton and Bachman, (1982)

$$V_p = 1952.5 - 86.26M_z + 4.14M^2_z. \quad (4)$$

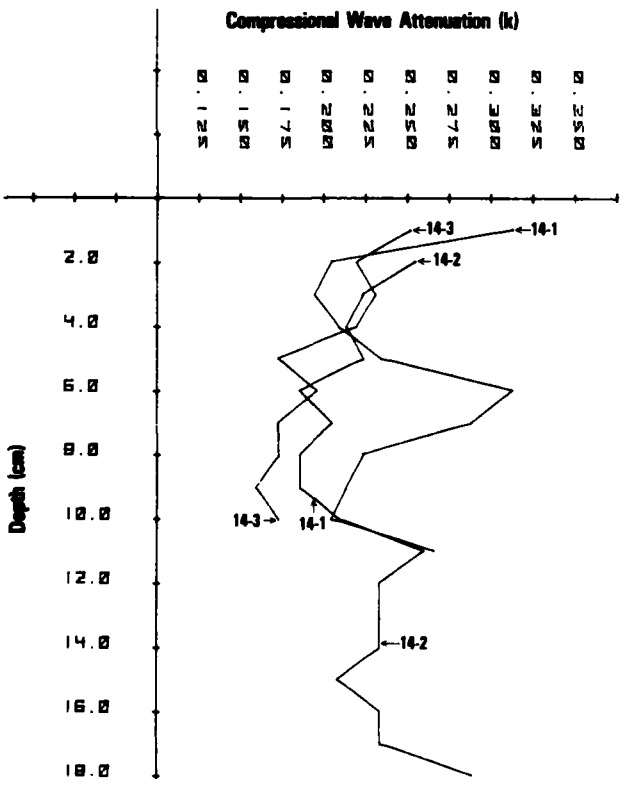

Figure 8. Vertical distribution of compressional wave attenuation (k) for three cores collected at Station 14

Compressional wave velocity was also measured directly at Station 14. All values are calculated for the approximate in-situ conditions of 6°C, 32.4 ppt salinity and 36 m water depth. Impedance was calculated as the product of density and compressional wave velocity.

The Rayleigh reflection coefficient (R) for compressional waves at normal incidence to the sediment-water interface

Table 3. Within-core and within-station variability of sediment geoacoustic properties for thirteen stations occupied during project WEAP

Core	Mean	#OBS	Variance	STD Dev
Mean Grain Size (Ø)				
2-1	0.03	10	0.07	0.26
2-2	0.18	8	0.07	0.26
3	2.45	6	0.00	0.27
4	2.89	7	0.54	0.74
5	2.48	5	0.00	0.02
9	2.21	6	0.00	0.05
11-1	0.68	9	0.02	0.15
14-1	2.08	7	0.0004	0.0195
14-2	2.01	11	0.0094	0.0970
14-3	2.07	7	0.0016	0.0400
14 (1-3)	2.067	25	0.0178	0.1333
Compressional Wave Velocity Ratio				
14-1	1.1434	11	0.00003	0.00579
14-2	1.1456	17	0.00007	0.00827
14-3	1.1258	9	0.00002	0.00455
14 (1-3)	1.1402	37	0.00011	0.01066
Compressional Wave Attenuation (k)				
14-1	0.238	11	0.0015	0.0393
14-2	0.225	17	0.0008	0.0276
14-3	0.192	9	0.0006	0.0248
14 (1-3)	0.2208	37	0.0012	0.0347
Porosity (%)				
14-1	37.79	7	0.085	0.291
14-2	35.69	10	0.619	0.787
14 (1-3)	36.55	17	1.510	1.229

was calculated as the impedance mismatch between water I(w) and sediment I(s) (Hamilton, 1970), where impedance (I) was the product of the compressional wave velocity and density of sediment or water.

$$R = \frac{I(s) - I(w)}{I(s) + I(w)} \quad (5)$$

Bottom loss (BL) was calculated in dB after Hamilton (1970)

$$BL = -20 \log R. \quad (6)$$

The fine sand sediments had lower mean density (2.01 vs 2.37 g/cm^3), compressional wave velocity (1698 vs 1878 m/sec), impedance (3.44 vs 4.46 $gcm^{-2}sec^{-} \cdot 10^5$) and Rayleigh reflection coefficient (0.39 vs 0.49 %) values and higher mean bottom loss (8.2 vs 6.2 dB) values than the coarse sand sediments.

Previous experiments (see Section D) suggest Hamilton's predicted compressional wave velocity values may be too high for coarse grained sediments. We,

Table 4. Measured and predicted surfical sediment geoacoustic properties for thirteen stations occupied during project WEAP. Mean grain size (Ø) values were measured while sediment density (ρ, g/cm^3), velocity ratio (V_p ratio), impedance [I, $(g/cm^2sec) \cdot 10^5$], Rayleigh reflection coefficient (R), and bottom loss (BL, dB) were predicted, except where footnoted.

Station	Ø	ρ	V_p*	I_s*	R	BL
2	0.04	2.367	1874	4.44	0.492	6.16
3	2.46	1.992	1697	3.38	0.382	8.36
4	2.50	1.987	1695	3.37	0.381	8.38
5	2.51	1.985	1694	3.36	0.380	8.40
6	-0.57	2.474	1926	4.76	0.518	5.71
7	2.14	2.036	1718	3.50	0.397	8.02
8	2.22	2.025	1713	3.47	0.394	8.09
9	2.23	2.024	1712	3.47	0.394	8.09
10	2.21	2.026	1713	3.47	0.394	8.09
11	0.58	2.275	1830	4.16	0.467	6.61
12	-0.12	2.395	1887	4.52	0.499	6.04
13	0.10	2.357	1869	4.41	0.490	6.20
14**	2.10	2.042	1721	3.51	0.398	8.00
14	2.10	2.050	1662	3.41	0.386	8.27
Coarse*** Sand	0.00	2.374	1728	4.10	0.462	6.71

* Calculated at insitu conditions of 6°C, 32.4 ppt salinity and 36 m water depth.

** Density (ρ) calculated from measured porosity values and compressional wave velocity (V_p) directly measured.

*** Mean Predictions for coarse sand sediments based on a compressional wave velocity of 1728 (see text). (Stations 2, 6, 11, 12, and 13).

therefore, calculated sediment geoacoustic properties based on a mean compressional wave velocity of 1728 m/sec. The coarse grained sediments (Stations 2, 6, 11, 12, and 13) then had a predicted sediment impedance of 4.10 $gcm^{-2}sec \cdot 10^5$, a Rayleigh reflection coefficient of 0.46%, and a bottom loss of 6.7 dB at normal incident.

At Station 14, bottom loss and Rayleigh reflection coefficients predicted given mean grain size were the same as bottom loss and reflection coefficients calculated directly from porosity and compressional wave velocity measurements. We, therefore, made no attempt to calculate different sediment geoacoustic properties than those predicted by mean grain size at stations with fine grained sediments (Stations 3, 4, 5, 7, 8, 9, and 10).

The attenuation of compressional waves (α) in sediments at frequencies used in the experiment can be calculated if the exponent of frequency (n) in equation (2) is assumed to be 1 (Hamilton, 1972). Mean attenuation at Station 14 was 88 dB/m at 400 kHz for a k value of 0.22. There were no apparent trends with depth. Acoustic forward scattering experiments in WEAP utilized transmit frequencies of 5, 10, 15, and 20 kHz and backscattering experiments utilized transmit frequencies of 5, 10, 15, 20, 40, and 80 kHz. At those frequencies the sediment attenuation would be 1.10 dB/m @ 5 kHz, 2.20 dB/m @ 10 kHz, 3.31 dB/m @ 15 kHz, 4.41 dB/m @ 20 kHz, 8.82 dB/m @ 40 kHz, and 17.64 dB/m @ 80 kHz. These attenuation values are also probably good estimates for the attenuation at Stations 3, 4, 5, 7, 8, 9, and 10.

Attenuation measurements were not made at the coarse sand stations and are outside the limits of Hamilton's (1972, 1980) predictor equations. Using the results of this experiment, attenuation measurements off Mission Beach, California, (Richardson et al., 1983b) and extrapolating Hamilton's (1980) graphic attenuation data, a k value of between 0.15 to 0.20 seems reasonable. Sediment attenuation values would therefore be 10 to 30% lower at coarse sand stations (2, 6, 11, 12, and 13) compared to fine sand stations.

C. Correlation Between Sediment Geoacoustic Properties

Correlations between sediment geoacoustic properties were restricted to data collected at Station 14. Attenuation values were not correlated with any other measured geoacoustic property while porosity (%) and compressional wave velocity had a weak (90%) negative correlation (Fig. 9). Sediment mean grain size was negatively correlated with compressional wave velocity ration at the 99.9% level and positively correlated with porosity at the 99% level. Although these correlations correspond to other empirical relationships (Hamilton, 1980, Hamilton and Bachman, 1982), the narrow range of geoacoustic values in this data set preclude any meaningful conclusions.

D. Comparison with Geoacoustic Predictor Equations

Numerous empirical predictor equations between sediment acoustic and physical properties have been developed by the simultaneous measurement of both properties (Nafe and Drake, 1963; Horn et al., 1968; Buchan et al., 1972; and Anderson, 1974, for example). The most recent and comprehensive are those of Hamilton and Bachman (1982) for prediction of compressional wave velocity and Hamilton (1980) for prediction of attenuation. Comparisons between Hamilton's predictor equations and our measured values for Station 14 are presented in Table 5.

Predicted compressional wave velocity ratios were 3-5 percent higher than measured values. This is equivalent of a 55-93 m/sec higher predicted compression wave velocity and translates into a higher predicted sediment impedance and Rayleigh reflection coefficient and a

lower predicted bottom loss than those more directly measured (Table 4). Although not measured it was estimated that the predicted bottom loss for the coarse sand sediments was 8 percent too high.

Predicted attenuation values were more than double those actually measured. Measured values were outside the envelope of predicted attenuation from Hamilton (1980).

Table 5. Comparison of measured and predicted sediment acoustic properties for sediments collected at Station 14. Predicted values based on equations given by Hamilton and Bachman (1982) and Hamilton (1980).

Geoacoustic Property	Measured	Predicted Given Mean Grain Size	Predicted Given Porosity
Compressional wave velocity ratio	1.1402	1.171	1.197
Attenuation (k)	0.22	0.51	0.47
Porosity (%)	36.6	39.6	--

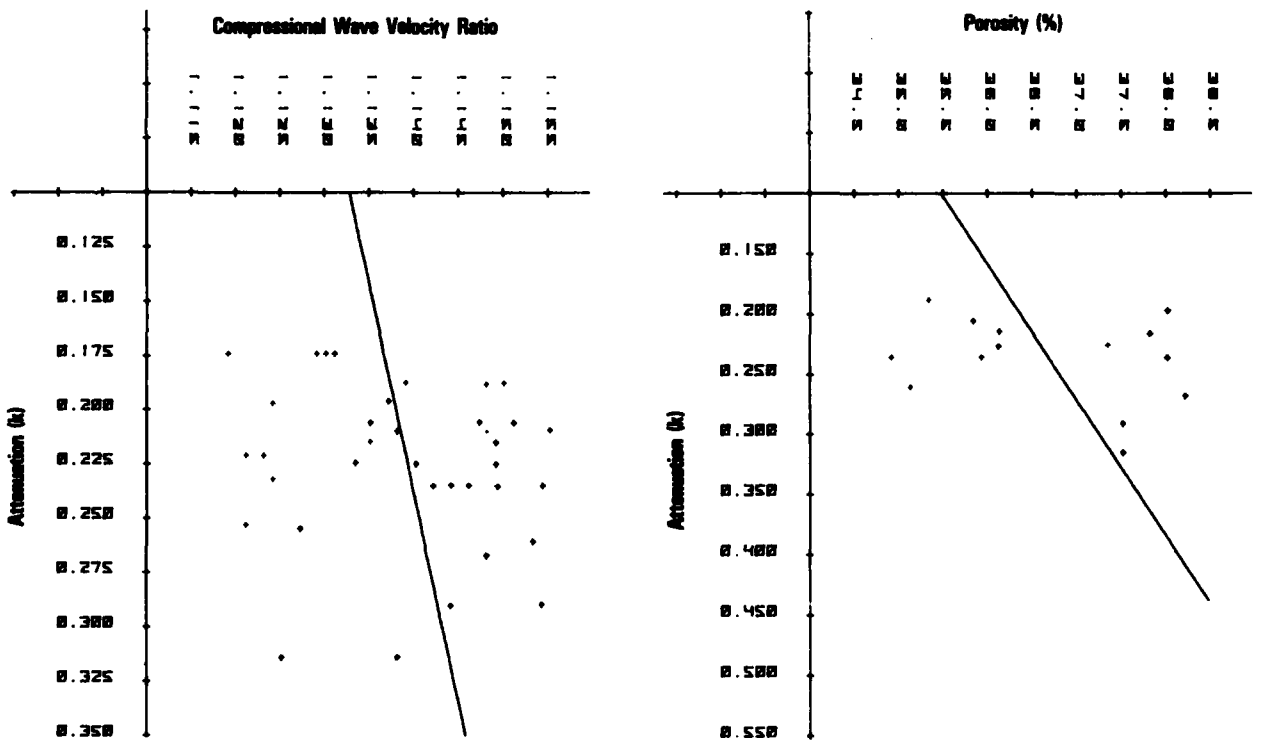

a) attenuation with velocity ratio

b) attenuation with porosity

Figure 9. Regressions of sediment geoacoustic properties for three cores collected at Station 14

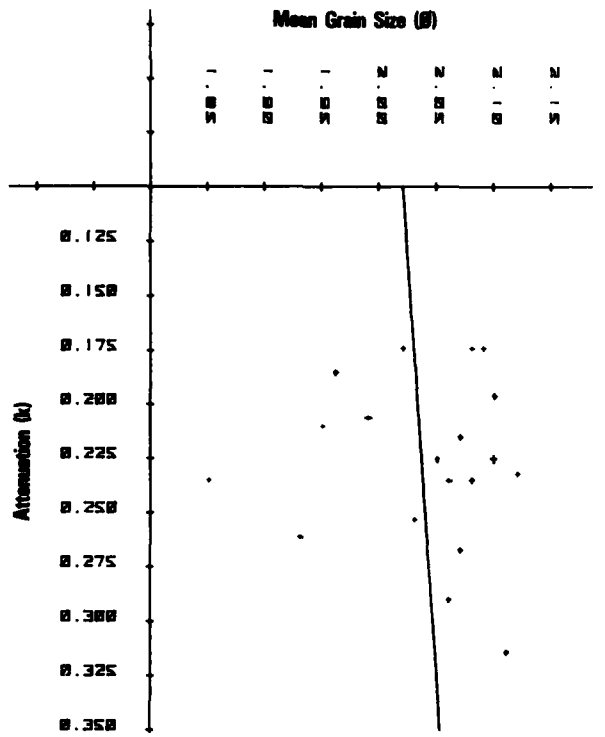

c) attenuation with mean grain size

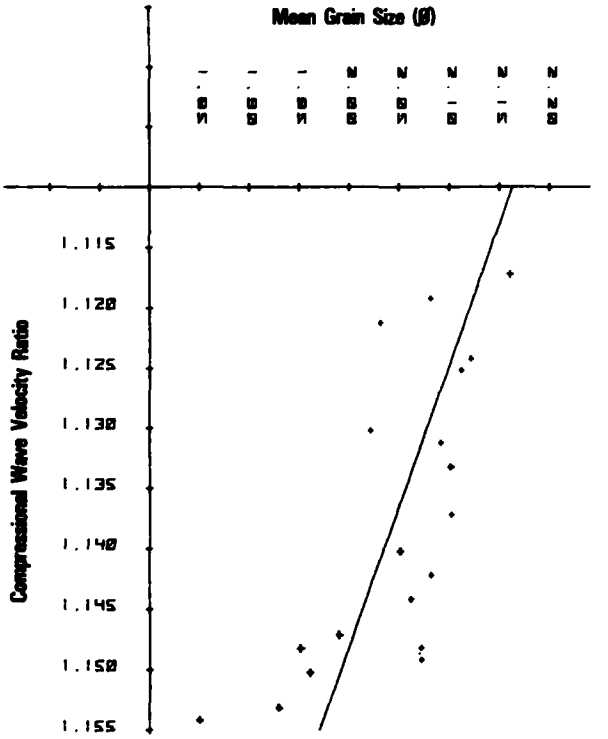

d) velocity ratio with mean grain size

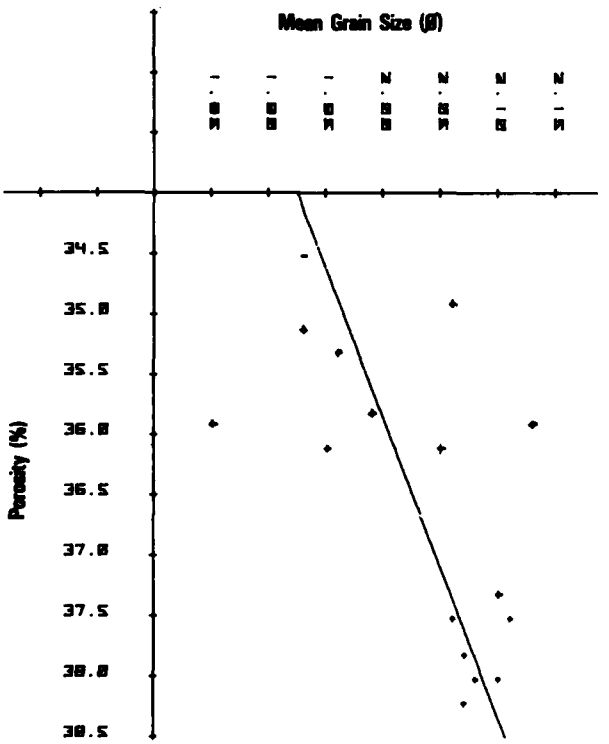

e) porosity with mean grain size

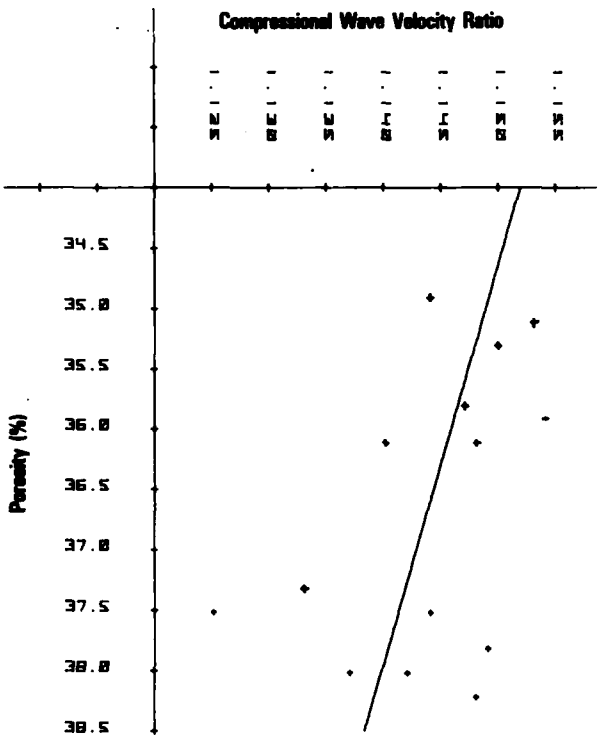

f) porosity with velocity ratio

Figure 9, (continued). Regressions of sediment geoacoustic properties for three cores collected at Station 14

Part B: Species Composition, Abundance and Biomass of Macrobenthos

John H. Tietjen

I. Introduction

The objective of this phase of the project was to provide qualitative and quantitative information of the distribution of macrobenthic animals in the experimental test site. Correlations of the acoustical properties of the sediments with animal distributions will be made in Part C.

II. Methods

Twelve samples were taken aboard the USNS LYNCH on 25 May 1982 with a 0.025 m^2 box corer (Table 1, Fig. 3). Sediments were washed on board ship through a 0.500 mm mesh sieve and preserved in 5% buffered sea water-formalin. Identifications were made to lowest identifiable taxon. Wet weights of the animals were measured by blotting individual animals in paper towels and weighing them on a Mettler HS microbalance (± 1 μg).

III. Results and Discussion

The estimated population densities per m^2 and relative abundances of all animals identified are given in Table 6. Population densities per m^2 ranged from 440 (Station 13) to 6000 (Station 12). Annelids and anthropods were the most abundant phyla at most stations, but echinoderms (specifically the sand dollar, Echinarachnius parma) were dominant at Stations 3, 8, and 10 (Table 7).

Biomass (g wet wt. m^{-2}) of the macrofauna is given in Table 8. Because of their large average weight (2.62 gm), Echinarachnius parma individuals contributed significantly to benthic biomass at those stations where they were present. At Station 4, for example, where they numbered 600 per m^2, sand dollar biomass was 1572 gm/m^{-2}. At Stations 3, 8, and 10, their contribution to macrofaunal biomass averaged 92% of the total. Arthropods, represented mainly by ampeliscid and haustoriid amphipods, while dominant numerically, were not very important in terms of biomass. Annelids (especially Clymenella torquata) were important contributors to biomass at those stations where E. parma populations were low or absent (Stations 6, 11, 12, and 13). Other large animals which contributed significantly to macrofauna biomass were Mercenaria mercenaria at Station 1, Edwardsia sp at Stations 5 and 12, and the hemichordate, Stereobalanus canadensis, at Stations 5, 6, and 10.

Twenty species had mean relative abundance of more than 1%; these are listed in Table 9. The sand dollar Echinarachnius parma appears to exert a dominant effect on the macrofauna of the area. An inverse correlation (Kendall's tau) between E. parma abundance, and polychaete ($T = -0.80$, $p < .01$) and crustacean ($T = -0.69$, $p < .05$) abundances existed at the study site. Furthermore, at those stations where E. parma accounted for more than 3% of the total individuals present (Stations 1, 3, 4, 7, 8, and 10), the densities of polychaetes and crustaceans were significantly lower than at those stations (Stations 6, 11, 12, and 13) where E. parma densities were less than 1% (Mann-Whitney U test, $p < .05$). Given the average wet weight (2.62 gm) and surface area (10 cm^2) of the E. parma individuals collected in the study area, their dominant position in the macrofaunal community is apparent.

Faunal affinities among the stations were examined employing the Bray and Curtis (1957) similarity coefficients which were clustered using group average sorting (Fig. 10). At least two major clusters of stations exist: those at which Echinarachnius parma densities are less than 1% (Stations 6, 11, 12, and

Table 6. Species composition of the macrobenthos at each station in the Project WEAP site, 25 May 1982. First number represents number per m^2 (observed 0.025 m^2 x 40), number in parenthesis represents percent of total.

Species	STATION											
	1	3	4	5	6	7	8	9	10	11	12	13
Hydrozoa												
Pennaria sp	40(1.5)			40(1.0)	40(0.8)			40(0.9)	80(5.6)		40(0.7)	
Unidentified spp											40(0.7)	
Anthozoa												
Edwardsia sp	40(1.5)			40(1.0)							40(0.7)	
Rhynchnocoela												
Unidentified sp		40(2.4)							40(2.8)			
Mollusca												
Mercenaria mercenaria	80(3.1)											
Pitar morrhuana			40(2.8)									
Musculus corrugatus								40(0.9)		120(2.2)		
Polychaeta												
Clymenella torquata	200(7.7)	40(2.4)	80(8.6)	160(3.9)	520(10.6)	40(7.7)	120(7.3)	40(0.9)	40(2.8)	1680(31.6)	120(2.0)	80(18.2)
Drilonereis magna	80(3.1)			40(1.0)						120(2.2)	40(0.7)	120(27.3)
Drilonereis longa	160(6.2)				1120(22.9)							
Eteone lactea	40(1.5)							80(1.7)		40(0.8)	80(1.3)	
Goniada maculata	40(1.5)				960(19.7)					1240(23.3)	240(4.0)	40(9.1)
Syllis gracilis	40(1.5)											
Harmothoe imbricata	40(1.5)											
Glycera capitata	40(1.5)			40(1.0)		80(15.3)	40(2.4)	40(0.9)		880(16.5)	320(5.4)	40(9.1)
Laonice cirrata	40(1.5)	120(7.1)	200(14.3)	160(3.9)	440(9.0)	40(7.7)	120(7.3)	80(1.7)	120(8.3)			
Brania sp		40(2.4)			80(1.6)							
Scalibregma inflatum			40(2.8)	40(1.0)				40(0.9)				
Onuphis eremita					240(4.9)							
Cirriformia filigera					40(0.8)							
Phyllodoce mucosa					40(0.8)			40(0.9)				
Scoloplos armiger					40(0.8)	40(7.7)					40(0.7)	
Lepidonotus squamatus					40(0.8)					40(0.8)		

Table 6. (continued). Species composition of the macrobenthos at each station in the Project WEAP site, 25 May 1982. First number represents number per m^2 (observed 0.025 m^2 x 40), number in parenthesis represents percent of total.

Species	STATION											
	1	3	4	5	6	7	8	9	10	11	12	13
Spionidae					160(3.3)					40(0.8)		40(9.1)
Nephtyidae						40(7.7)						
Microphthalmus aberrans							40(2.4)	40(0.9)				
Pygospio elegans											200(3.3)	40(9.1)
Syllides sp											40(0.7)	
Scolepis squamata											160(2.7)	
Lumbrinereis sp											40(0.7)	
Aricidea catherinae												80(18.2)
Sipuncula												
Unidentified sp										40(0.8)		
Crustacea												
Hutchinsoniella macracantha					40(0.8)							
Eudorellopsis deformis	80(3.1)	40(2.4)	160(11.4)				160(2.4)	120(2.6)	40(2.8)			
Diastylis sculpta	40(1.5)											
Leptostylis ampullacea	40(1.5)											
Diastylis quadrispinosa			40(2.8)									
Edotea triloba	80(3.1)				40(0.8)					120(2.2)		
Cyathura burbancki	40(1.5)	80(4.8)		80(2.0)			120(7.3)	120(2.6)				
Cirolana polita		40(2.4)		40(1.0)				80(1.7)		40(0.8)		
Ampelisca verrilli	200(7.7)			800(19.6)			120(7.3)	1080(23.3)	120(8.3)	40(0.8)		
Ampelisca vadorum	80(3.1)			40(1.0)				120(2.6)	120(8.3)			
Ampelisca agassizi	120(4.6)			1240(30.4)			120(7.3)	1280(27.6)	160(11.1)			
Byblis serrata			120(8.6)	400(9.8)				80(1.7)				
Orchomonella minuta	160(6.2)	120(7.1)	40(2.8)	480(11.8)	840(17.2)		160(9.8)	320(6.9)			1480(24.8)	
Anonyx sarsi					40(0.8)						80(1.3)	
Acanthohaustorius millsi	120(4.6)	280(16.7)					320(19.5)		240(16.7)			
Protohaustorius wigleyi	600(23.1)								120(8.3)		40(0.7)	

Table 6, (continued). Species composition of the macrobenthos at each station in the Project WEAP site, 25 May 1982. First number represents number per m^2 (observed 0.025 m^2 x 40), number in parenthesis represents percent of total.

Species	STATION											
	1	3	4	5	6	7	8	9	10	11	12	13
Parahaustorius attenuatus		200(11.9)										
Pseudohaustorius carolinensis			80(5.7)	40(1.0)				240(5.2)				
Corophium bonelli	40(1.5)	80(4.8)		200(4.9)				80(1.7)			160(2.7)	
Uniciola irrorata								200(4.3)		40(0.8)	360(6.0)	
Calliopius laeviusculus											200(3.3)	
Stenothoe minuta				80(2.0)	40(0.8)			360(7.8)		560(10.5)	1280(21.5)	
Trichophoxus epistomus		80(4.8)										
Microdeutopus gryllotalpa					120(2.4)				40(2.8)	80(1.5)	400(6.7)	
Casco bigelowi										120(2.2)		
Stenopleustes inermis											560(8.7)	
Echinodermata												
Echinarachnius parma	80(3.1)	360(21.4)	600(42.9)	80(2.0)		280(53.8)	280(17.1)	80(1.7)	240(16.7)	40(0.8)		
Bryozoa												
Crisia eburnea								40(0.9)		80(1.5)	40(0.7)	
Unidentified sp	80(3.1)	80(4.8)		40(1.0)			40(2.4)		40(2.8)			
Hemichordata												
Stereobalanus canadensis		40(2.4)		40(1.0)	40(0.8)				40(2.8)			

Table 7. Quantitative distribution of population densities (observed 0.025 m^2 x 40) of major benthic invertebrate phyla at each station in the Project WEAP site, 25 May 1982. Numbers in parenthesis represent percent of total.

	STATION											
Phylum	1	3	4	5	6	7	8	9	10	11	12	13
Cnidaria	120 (4.5)			80 (2.0)	40 (0.8)			40 (0.9)	80 (5.6)		120 (2.0)	
Rhynchnocoela		40 (2.4)							40 (2.8)			
Mollusca	80 (3.0)		40 (2.8)					40 (0.9)		120 (2.3)		
Annelida	680 (25.8)	200 (11.9)	320 (22.8)	440 (10.8)	3680 (75.4)	240 (46.2)	320 (20.0)	360 (7.7)	160 (11.1)	3960 (75.6)	1280 (21.3)	440 (100)
Sipunculida										40 (0.8)		
Arthropoda	1600 (60.6)	920 (54.8)	440 (31.4)	3400 (83.3)	1120 (23.0)		1000 (61.0)	4080 (87.9)	840 (58.3)	1000 (19.1)	4560 (76.0)	
Bryozoa	80 (3.0)	80 (4.8)		40 (1.0)			40 (2.4)	40 (0.9)	40 (2.8)	80 (1.5)	40 (0.7)	
Echinodermata	80 (3.0)	360 (21.4)	600 (42.8)	80 (2.0)		280 (53.8)	280 (17.1)	80 (1.7)	240 (16.7)	40 (0.8)		
Hemichordata		80 (4.8)		40 (1.0)	40 (0.8)				40 (2.8)			
TOTAL	2640	1680	1400	4080	4880	520	1640	4640	1440	5240	6000	440

Table 8. The distribution of biomass (grams wet weight per m^2) of major benthic invertebrate phyla at each station in the Project WEAP site, 25 May 1982. Numbers in parenthesis represent percent of total.

	STATION											
Phylum	1	3	4	5	6	7	8	9	10	11	12	13
Cnidaria	464.0 (6.3)			172.8 (33.0)	<1			<1	<1		185.2 (49.4)	
Rhynchnocoela		3.3 (0.3)							3.7 (0.5)			
Mollusca	6560.0 (89.2)		144.0 (8.2)					40.4 (19.5)		121.2 (14.1)		
Annelida	103.3 (1.4)	20.2 (2.0)	34.9 (2.0)	67.6 (12.9)	382.2 (87.2)	33.8 (4.4)	40.3 (5.2)	34.1 (16.5)	17.8 (2.5)	601.1 (70.0)	158.5 (42.3)	491.1 (100.0))
Sipuncullida										21.5 (2.5)		
Arthropoda	11.0 (0.1)	6.6 (0.6)	2.1 (0.1)	21.9 (4.2)	5.0 (1.1)		5.4 (0.7)	27.1 (13.1)	6.6 (0.9)	6.5 (0.7)	30.6 (8.2)	
Bryozoa	<1	<1		<1			<1				<1	
Echinodermata	209.6 (2.8)	943.2 (92.1)	1572.0 (89.7)	209.6 (40.1)		733.6 (95.6)	729.5 (94.1)	104.8 (50.1)	628.6 (88.5)	107.6 (12.5)		
Hemichordata		51.2 (5.0)		50.3 (9.6)	51.2 (11.7)				53.5 (7.5)			
TOTAL	7347.9	1024.5	1753.0	522.2	438.4	767.4	775.2	206.4	710.2	857.9	374.3	491.1

Table 9. Abundance per square meter and percent of total (number in parenthesis) of the twenty most common species of macrofauna occurring in the sediments at the Project WEAP site, 25 May 1982

Species	STATION					
	1	3	4	5	6	7
Clymenella torquata	200(7.7)	40(2.4)	80(5.7)	160(3.9)	520(10.6)	40(7.7)
Drilonereis magna	80(3.1)			40(1.0)		
Drilonereis longa	160(6.2)				1120(22.9)	
Goniada maculata					960(19.7)	
Glycera capitata				40(1.0)		80(15.3)
Leonice cirrata		120(7.1)	200(14.3)	160(3.9)	440(9.0)	40(7.7)
Pygospio elegans						
Aricidea catherinae						
Eudorellopsis deformis	80(3.1)	40(2.4)	160(11.4)			
Cyathura burbancki		80(4.8)	80(5.7)	80(2.0)		
Ampelisca verrilli	200(7.7)			800(19.6)		
Ampelisca vadorum	80(3.1)			40(1.0)		
Ampelisca agassizi	120(4.6)			1240(30.4)		
Orchomonella minuta	160(6.2)	120(7.1)		480(11.8)	840(17.2)	
Acanthohaustorius millsi	120(4.6)	280(16.7)				
Protohaustorius wigleyi	600(23.1)	200(11.9)				
Corophium bonelli		80(4.8)		200(4.9)		
Stenothoe minuta				80(2.0)	40(0.8)	
Byblis serrata			120(8.6)	400(9.8)		
Echinarachnius parma	80(3.1)	360(21.4)	600(42.9)	80(2.0)		280(5.3)

Table 9, (continued). Abundance per square meter and percent of total (number in parenthesis) of the twenty most common species of macrofauna occurring in the sediments at the Project WEAP site, 25 May 1982

Species	STATION					
	8	9	10	11	12	13
Clymenella torquata	120(7.3)	40(0.9)	40(2.8)	1680(31.6)	120(2.0)	80(18.2)
Drilonereis magna				120(2.2)	40(0.7)	120(27.3)
Drilonereis longa						
Goniada maculata				1240(23.3)	240(4.0)	40(9.1)
Glycera capitata	40(2.4)	40(0.9)		880(16.5)	320(5.4)	40(9.1)
Leonice cirrata	120(7.3)	80(1.7)	120(8.3)			
Pygospio elegans					200(3.3)	40(9.1)
Aricidea catherinae					40(0.7)	
Eudorellopsis deformis	160(9.7)	120(2.6)	40(2.8)			
Cyathura burbanckl	120(7.3)	120(2.6)				
Ampelisca verrilli	120(7.3)	1080(23.3)	120(8.3)	40(0.8)		
Ampelisca vadorum		120(2.6)	120(8.3)			
Ampelisca agassizi	120(7.3)	1280(27.6)	160(11.1)			
Orchomonella minuta	160(9.7)	320(6.9)			1480(24.8)	
Acanthohaustorius millsi	320(19.5)		240(16.7)			
Protohaustorius wigleyi			120(8.3)		40(0.7)	
Corophium bonelli		80(1.7)			160(2.7)	
Stenothoe minuta		360(7.8)		560(10.5)	1280(21.5)	
Byblis serrata		80(1.7)				
Echinarachnius parma	280(17.1)	80(1.7)	240(16.7)	40(0.8)		

13) and those at which E. parma population densities are greater than 1% (Stations 1, 3, 4, 5, 7, 8, 9, and 10). Within the latter group, Stations 5 and 9 form a subgroup, based on the high abundances of Ampelisca verrilli and A. agassizi shared by both stations (Table 9). Station 12 was also dominated by amphipods, but the dominant species were different (Orchomonella minuta and Stenothoe minuta).

Macrofaunal species diversity was calculated from the Shannon-Wiener information function (H'), and species evenness by J' (Pielou, 1975). Species richness (SR) was estimated by SR = (S-1)/ln N, where S is the number of species and N the number of individuals in a sample (Margalef, 1958). Results are given in Table 10.

Species diversity (especially species richness) was lowest at Stations 4 and 7, at which the sand dollar, Echinarachnius parma, attained maximum dominance (50.0% and 46.2% of the total number of animals present at each station, respectively). At Stations 3, 8, and 10, E. parma constituted 20.9, 17.1 and 16.7% of the macrofauna present; however, diversity and richness values at these stations overlapped those at Stations 6, 11, 12, and 13, where E. parma comprised less than 1% of the macrobenthic populations. Thus it appears that extremely high abundances of E. parma may contribute to lower benthic diversity, perhaps by simply physically excluding other species from the area occupied by the sand dollars. No other obvious relationships between macrofaunal diversity, and the presence or absence of particular animal species, was observed at the WEAP stations.

In summary, the sediments in the area of Project WEAP were dominated numerically by the sand dollar, Echinarachnius parma, ampeliscid and haustoriid amphipods, and several polychaete species (Clymenella torquata, Goniada maculata, Laonice cirrata, and Glycera capitata). An inverse relationship between sand dollar abundance and the abundances of crustaceans and polychaetes was evident, and served to separate the sediment in the Project WEAP area into two major groups.

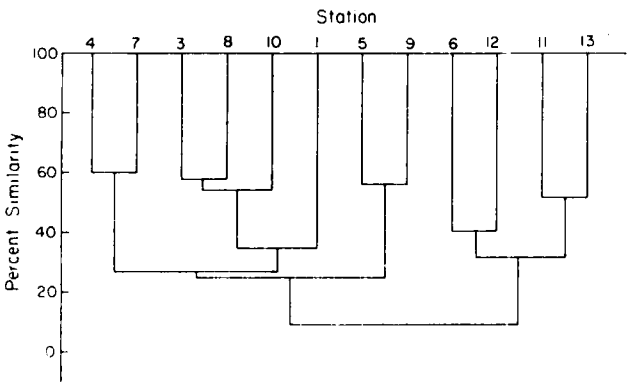

Figure 10. Dendrogram formed by group-average sorting of Bray-Curtis similarity values between all possible pairs of stations

Table 10. Species diversity (H'), evenness (J'), and richness (SR) of macrofauna collected at Project WEAP site, Block Island Sound, May 1982

Station	Species Diversity (H')	Evenness (J')	Species Richness (SR)
1	2.95	0.70	6.40
3	2.48	0.66	3.99
4	1.64	0.48	2.06
5	2.30	0.49	4.50
6	2.08	0.43	3.76
7	1.64	0.64	2.34
8	2.31	0.62	2.96
9	2.34	0.49	4.83
10	2.42	0.67	3.63
11	2.03	0.41	3.47
12	2.49	0.48	4.56
13	2.04	0.77	2.74

Part C: Discussion, Conclusions and Recommendations

Michael D. Richardson, John H. Tietjen

I. Effects of Biological Process on Sediment Geoacoustic Properties

The physical characteristics of marine sediments are profoundly affected by the activity of benthic organisms. This activity, bioturbation, includes burrowing, ingestion / digestion / defecation, tube building, biodeposition, cementation and metabolic activities (see Rhoads, 1974, for review). Bioturbation has been shown to influence the following properties of sediments, among others: porosity, mean grain size, and bulk density; compaction and cohesion; particle orientation and distribution; and microtopography (Richardson and Young, 1980). Bioturbation by benthic animals has also been shown to alter the acoustic properties of marine sediments by their direct effect on sediment physical properties and by their influence on erosional and depositional events (Richardson et al., 1983a).

We examined the biology of the dominant species collected on both substrate types at the WEAP site to determine the possible effects of bioturbation on sediment geoacoustic properties. We have also examined stereophotographs supplied by W. I. Roderick (NUSC) for possible effects of biological processes on sediment microtopography or bottom roughness.

Bioturbation at fine sand stations (3, 4, 5, 7, 8, 9, and 10) was dominated by macrofauna of two contrasting life styles (Table 11). The most obvious contribution to sediment reworking was by the surface deposit feeding sand dollar Echinarachnius parma. E. parma individuals burrow just below the sediment surface, feeding on faunal and detrital material (Fig. 11a). Parker (1927) and Parker and Van Alstyne (1932) found that E. parma buries by creating mounds of sand and burrowing in (Fig. 11b). Sand dollars right themselves by working anterior ends into the sediment, gradually erecting into a vertical position and falling over, ventral side down (Fig. 11c). All these activities mix the upper few centimeters of sediment thereby changing sediment geoacoustic properties and creating and destroying sediment microtopography. E. parma is also part of the microtopography occurring at different angles (Fig. 11c) and packed so densely that they occur on top of each other (Fig. 11d).

The second lifestyle was filter feeding by tube dwelling amphipods (Ampelisca verrilli, A. vadorum, A. agassizi, Byblis serrata, Microdeutopus gryllotalpa, Uniciola irrorata and Corophium bonelli) and polychaetes (Laonice cirrata). Numerous tubes of these species extend above the sediment-water interface (Fig. 12). All these species feed either by filtering particles from the overlying water or selecting faunal or detrital particles from the sediment surface (epistratal feeding). Suspension feeding can act as a mechanism to increase sedimentation of fine grained silts and clays thus changing sediment properties (Mills, 1967). Tubes can also change the hydrodynamic environmental at the sediment-water interface. The presence of high densities of tubes has been shown to stabilize (Fager, 1964; Mills, 1967; Myers, 1977b) and destabilize (Eckman et al, 1981) the sediment, and alter the distribution of benthic communities by exclusion (Woodin, 1974) or recruitment (Eckman, 1983). The presence of tubes also increases the small scale microtopography or bottom roughness.

As seen in Figures 11 and 12, the distribution of sand dollars, (Echinarachnius parma), and amphipod and polychaete tubes was patchy. Negative correlation between the densities of E. parma and polychaete and crustacean abundances reflects interaction between these two life styles. Reworking of the sediment by feeding and locomotion activities of

Table 11. Life history data for the twenty most abundant species collected at the WEAP experimental site, 25 May 1982.

Species	Purchase Type	Feeding Type	References
Polychaeta			
Clymenella torquata	infauna-tube	deep non-selective deposit	1,8
Drilonereis magna	infauna-free	carnivore	1
Drilonereis longa	infauna-free	carnivore	1
Goniada maculata	infauna-free	carnivore	1
Glycera capitata	infauna-free	detritivore-carnivore	1
Laonice cirrata	epifauna-tube	surface deposit	1
Cumacea			
Eudorellopsis deformis	infauna-free	selective deposit filter feeder	7
Isopoda			
Cyathura burbanckl	infauna-free	deposit feeder-carnivore	5,6
Amphipoda			
Ampelisca verrilli	epifauna-tube	filter surface	10
Ampelisca vadorum	epifauna-tube	filter surface	2
Ampelisca agassizi	epifauna-tube	filter surface	10
Bybis serrata	epifauna-tube	filter surface	11
Microdeutopus gryllotalpa	epifauna-tube	surface deposit feeder	5,6
Unciola irrorata	epifauna-tube	selective deposit	3
Corophium bonelli	epifauna-tube	surface deposit feeder	12
Acanthohaustorius millsi	infauna-free	deposit filter feeder	12
Protohaustorius wigleyi	infauna-free	deposit filter feeder	11
Orchomenella minuta	epifauna-free	scavenger	7
Stenothoe minuta	epifauna-free	scavenger	11
Echinodermata			
Echinarachnius parma	epifauna-free	selective deposit	4

(1) Fauchald and Jumars (1979)
(2) Mills (1967)
(3) Sanders (1960)
(4) Pearse et. al (1981)
(5) Myers (1977,a)
(6) Myers (1977,b)
(7) Barnes (1980)
(8) Rhoads (1963)
(9) Wigley and Therous (1981)
(10) Caracciolo and Steimel (1983)
(11) Dickinson and Wigley (1981)
(12) Bousfield (1973)

a. sand dollars burrowing just below the surface

b. sand dollars creating mounds by burrowing activity

10 cm

c. sand dollar righting

d. dense concentrations of sand dollars

Figure 11. Photographs of Echinarachinus parma, (sand dollar) burrowing activities at the WEAP experimental site.

E. parma destroys the stable beds of dense amphipod and polychaete tubes while predation by adult amphipods and polychaetes reduces the recruitment of newly settled sand dollar larvae. The interplay of those two life styles together with geological and hydrodynamic processes (next section) maintain the patchy distribution of these two groups of benthos.

Surface objects that have dimensions longer than the acoustic wave length are important scatterers of acoustic energy. Wavelengths for compressional waves traveling at 1471 m/sec for the frequencies used for this experiment (5-80 kHz) range from 29.4 to 1.8 cm. It is apparent that individual sand dollars, (E. parma) with a mean diameter of 3.5 cm (range 2.5 to 4.1 cm) were important surface point scatterers at 80 kHz and probably 40 kHz. It is doubtful that individual tubes of amphipods and polychaetes, with the longest dimension of about 0.5 cm, were important sound scatterers in Project WEAP.

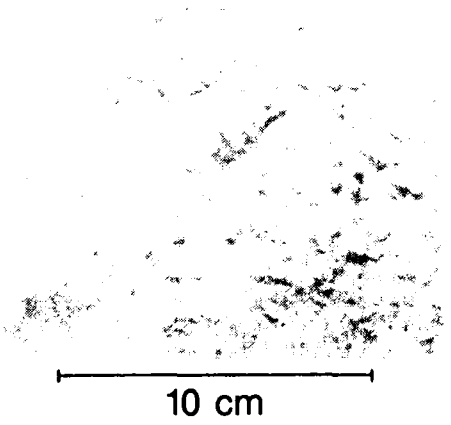

Figure 12. Photographs of tube dwelling amphipods at the WEAP experimental site

Sand dollars occurred in patches with densities so great as to create an overlapping "pavement" of live animals (Fig. 11). These patches, as large as the areal coverage of the photographs, may act as single point scatterers and be important for all frequencies used in these experiments.

The sediment microtopography created by E. parma includes a patchy distribution of mounds and depressions that were only slightly larger than the sand dollars. These features may cause resonance scattering. Fine scale roughness with wavelengths of $\lambda/2 \cos \theta$ (θ, grazing angle; λ, acoustic wavelength) cause most resonance scattering. At the 1 - 10° grazing angles important for this experiment, resonance scattering would be important for bottom roughness wavelengths of 15 cm at 5 kHz and 1 cm at 80 kHz.

It is not known if the density of tube dwelling amphipods and polychaetes is high enough to profoundly change the stability or physical properties of fine sand sediments. The highest densities of surface tube dwelling macrofauna were found at Stations 5 and 9 (approximately 750 individual/m^2). Mills (1967), Fager (1964), Wooden (1976) and others have found much higher densities of tube dwellers. Densities of tube dwellers derived from photographs also suggest the maximum density of tube dwellers has not been reached. Analysis of grain size distribution shows no enrichment of silt or clay size particles in the upper few centimeters of sediments as might be expected if suspension feeders were depositing material at the sediment-water interface.

These observations suggest that in the fine sand sediments, bioturbation by E. parma is the most important biological process relative to sediment microtopography and surface scattering characteristics.

The coarse sand stations (6, 11, 12, and 13) were dominated by free-living carnivorous polychaetes (Drilonerís magna, D. longa, Goniada maculata, and Glycera capitala) and the deep non-selective deposit feeding polychaete Clymenella torquata. It is doubtful that the free burrowing polychetes would have a major impact on microtopography or sediment geoacoustic properties, but the tube-dwelling polychaete Clymenella torquata has been reported to have major influence on sediment properties (Rhoads, 1963, 1967; Mangum, 1964; Aller, 1978). Specimens of C. torquata normally inhabit sandy substrates along the east coast of North America. These maldanids orient vertically in their tubes ingesting sediment at depth and depositing it on the surface (Mangum, 1964). This "conveyer belt feeding" (Sensu and Rhoads, 1974), is known to alter the chemical (Aller, 1978) and physical environment (Rhoads, 1963). Specimens of C. torquata not only mix the sediments, creating voids and other heterogeneities at depth, but create considerable surface microtopography (Rhoads, 1967). Although no visual or photographic observations were made of sediments containing C. torquata (Stations 6 and 11 in particular), the large size and high densities suggest this polychaete could be responsible for considerable surface roughness and geoacoustic heterogenity. Rhoads (1967) calculated a sediment turnover rate of 274 ml/yr for individuals of C. torquata. The volume of sediment turned over each year would therefore be 460 liters at Station 11 (274 ml x 1680 worms), which is more than double the volume occupied by 1680 polychaetes. The time required for 1680 worms to cycle 200 liters of sediment (the volume of sediment occupied by the worms) is calculated to be 0.42 yr.

II. Effects of Physical Process on Sediment Geoacoustic Properties

The inner continental shelf of the middle Atlantic Bight is covered by a vast sand plain (Swift et al., 1973). The first-order (shelf valleys, massifs, cuestas, and terraces) and second-order (ridge and swale topography) morphologic features are well-charted and their formation understood (Duane et al., 1972; Swift, et al., 1972; Swift et al., 1973; Schlee, 1973; Freeland and Swift, 1978). It should, thefore, be possible to predict sediment geoacoustic propertics from the distribution of these first and second order features.

Unfortunately, the experiment was sited at the southern terminus of a drowned barrier spit. The drowned barrier spit-lagoon-headland complex described by McMaster and Garrison (1967) is a very complex sedimentary area. The distribution of surfical sediment in this area is controlled by historical and modern processes. The iron-oxide rich coarse sand is a relict lag deposit of glacial origin. It is probable that large symmetrical ripples found in the coarse sediment are in dynamic equilibrium with major storm events, which are common along the east coast.

The fine sand sediments are similar to most sediments found on the middle Atlantic sand plain described by Schlee (1973) and Freeland and Swift (1978). These sediments are well-sorted and similar to beach sand from the Atlantic coast. The sand was probably deposited during previous glacial regressions but is in dynamic equlibrium with present hydrological conditions. The sand ridges formed of these well-sorted sands migrate during the periodic severe storms. The size and location of these ripples probably change with season, as does the the interface between coarse and fine sand. Side scan imagery techniques were required to delineate the distribution of both sediment types at the time of the experiment. Had the experiment been sited in water 10 m deeper we believe the sediment geoacoustic properties would have been predictable. Sediment would have had the same geoacoustic properties as the fine sand described in this report. Sediment microtopography could have been predicted from recent meteorological data coupled with a

knowledge of the distribution of benthic fauna.

III. Recommendations for Future Experiments

Basic physical and empirical submodels are required to extrapolate acoustic bottom reverberation prediction beyond the measured acoustic data bases. One of the important goals of this project was to collect the high quality acoustic and environmental data required for this submodel development and verification. Ideally, these data should be collected from the same location and as close to the same time as possible. The narrow beam-width and absence of side lobes of the acoustic signals generated by NUSC parametric source make this system ideal for this data collection. The area insonified is small, and its exact location known. Acoustic parameters such as frequency, pulse length, and grazing angle can be easily controlled.

Two philosophies of environmental data collection could have been used to generate the required environmental data. The first philosophy would be to determine the statistical variability of environmental parameters (seafloor roughness; sediment mean grain size, density, porosity; compressional wave velocity and attenuation of sediment; distribution and abundance of fauna) for the insonified area. These data could then be compared to the complex envelope statistics for the scattered acoustic signals for each frequency, pulse length, and grazing angle used in the experiment without regard to actual location of the insonified area. This philosophy of data collection requires that the variability of acoustic and environmental data be low enough to generate submodels with the precision required for weapon system design.

The second philosophy would be to determine the distribution of values of environmental parameters for the entire insonified area. Environmental and acoustic data could then be compared for each patch insonified. The variability of acoustic and environmental data within each patch must still be low; the grain of patch size of acoustic and environmental data must be matched.

The WEAP site was chosen for its homogeneity in sediment properties, so, the first philosophy was selected. Unfortunately, as seen from these data, such was not the case. The WEAP site contained a patchy distribution of two different substrate types with different biological, geoacoustic, and sediment roughness properties. With the equipment and time available it was impossible to employ the second philosophy and determine the distribution of values of environmental parameters for the entire insonified area. The following recommendations are, therefore, made for future experiments.

An extensive presite survey of possible experimental sites is required. Large scale mapping of major sediment types is best accomplished using side-scan sonar classification techniques in combination with remote underwater television observations and remote sediment sampling for ground truthing. After the experimental site has been chosen, direct sampling to determine the variability of sediment biological, geoacoustic, and sediment roughness properties is required. In-situ probes are the best sampling techniques for sediment geoacoustic properties. Remote sampling with box cores can also be used to collect relatively undisturbed sediment samples for geoacoustic measurements. Considerable attention must be paid, not only to surficial sediment geoacoustic properties, but to the presence of inhomogeneities and point scatterers within the sediment.

Direct observations and data collection by (scuba) divers are preferred to remote sampling when possible. If the water depth is beyond scuba divers' range, remote in-situ sampling monitored by underwater television cameras can be effective. Insight into biological and bottom roughness characteristics can be determined both by scuba divers and by

underwater television observations. These techniques cover different patch sizes and both should be used when possible.

Analyses of all data and observations from the presite survey can be used to site the experiment in a homogeneous area or at least in an area where heterogeneities can be predicted and mapped. It is important that the patch size of sediment types in heterogeneous areas is much larger than the size of the insonified area. It is preferable to conduct a series of experiments in different but homogeneous areas compared to complex areas with a variety of sediment types.

During or after the acoustic experiment, an extensive environmental site characterization is required. Physical and empirical geoacoustic submodels require the input parameters listed in Table 12 to predict acoustic backscatter and forward scattering. Not all models require all parameters as inputs although as many as possible should be measured so different or new submodels can be developed and validated. If the bottom is relatively homogeneous, data collection should concentrate on determining the depth distribution and horizontal variability of these parameter values. More samples will be required to determine the within-patch variability if the bottom is heterogeneous. Side-scan sonar mosaics can then be used to determine the distribution of patches so acoustic and environmental data can be compared for the same patch.

As with the presite survey, in-situ sampling of sediment geoacoustic properties with scuba diver operated probes is best. Remote in-situ sampling can be monitored by underwater television cameras in deeper water. Scuba diver collected sediment samples are preferred if in-situ probes are not availble. Box core type samplers collect the least disturbed samples in deeper water.

Sediment microtopography can be determined from overlapping stereophotographs, sediment acoustic microprofilers, or hand operated profilers. Overlapping stereo-photographs and acoustic microprofilers generate more detailed data but can be quite expensive.

Biological samples can be collected with diver operated or remotely collected box cores for small macrofaunal animals. Megafauna must be collected with nets or observed by scuba divers or underwater television. The insights of trained benthic ecologists are required to interpret this type of data. Laboratory experiments using dominant species found in the study area may be required to determine the rates and types of bioturbation by both megafauna and macrofauna. This data may be required to understand the effects of these animals on sediment geoacoustic properties and microtopographic features.

Table 12. Environmental input parameters for physical and empirical geoacoustic submodels

I.	Sediment Physical Properties
A.	Porosity
B.	Grain size distribution statistics
C.	Density
D.	Compressional wave velocity and attenuation
E.	Shear wave velocity and attenuation
F.	Surface point scattering strength and distribution
G.	Volume scattering strength and distribution
H.	Bottom impedance
I.	Faunal densities and distribution
J.	Rates of bioturbation
K.	Permeability
L.	Percent organic carbon
M.	Percent $CaCO_3$
N.	Shear strength
II.	Sediment topography
A.	Slope probability density
B.	RMS roughness
C.	Power spectrum of fine scale bottom roughness

References

Aller, R. C. (1978). Experimental Studies on Changes Produced by Deposit Feeders on Pore Water, Sediment, and Overlying Water Chemistry. Am. J. Sci. v. 278, pp. 1185-1234.

Anderson, R. S. (1974). Statistical Correlation of Physical Properties and Sound Velocity in Sediments. In: L. Hampton (ed.) Physics of Sound in Marine Sediments. pp. 481-518. Plenum Press, New York, N.Y.

Barnes, R. D. (1980). Invertebrate Zoology, 4th Edition. Saunders College, Philadelphia, Pa.

Bousfield, E. L. (1973). Shallow Water Gammaridea-Amphipoda of New England. Cornell Univ. Press, Ithaca, N.Y. 313 pp.

Bray, R. J. and J. T. Curtis (1957). An Ordination of the Upland Forest Communities of Southern Wisconsin. Ecol. Monogr., vol. 27, pp. 325-349.

Buchan, S., D. M. McCann and D. T. Smith (1972). Relations Between the Acoustic and Geotechnical Properties of Marine Sediments. Q. J. Engng. Geol. v. 5, pp. 265-284.

Caracciolio, J. V. and F. W. Steimle, Jr. (1983). An Atlas of the Distribution and Abundance of Dominant Benthic Invertebrates in the New York Bight Apex, with Reviews of Their Life Histories. U.S. Dept. Commerce, NOAA Tech Rept., NMFS SSRF-766. 58 pp.

Dickinson, J. J. and R. L. Wigley (1981). Distribution of Gammaridean Amphipoda (Crustacean) on Georges Bank. U.S. Dept. Commerce, NOAA Tech. Rep., NMFS SSRF-746. 25 pp.

Duane, D. B., M. E. Field, E. P. Meisburger, D. J. P. Swift and S. J. Williams (1972). Linear Shoals on the Atlantic Inner Continental Shelf, Florida to Long Island. In: Swift, D. J. P., D. B. Duane and O. H. Pilkey (eds.), Shelf Sediment Transport: Process and Pattern. Dowden, Hutchinson and Ross, Stroudsburg, Pa. pp. 447-498.

Eckman, J. E. (1983). Hydrodynamic Processes Affecting Benthic Recruitment. Limnol. Oceanogr. v. 28, pp. 241-257.

Eckman, J. E., A. R. M. Newell and P. A. Jumars (1981). Sediment Destabilization by Animal Tubes. J. Mar. Res. v. 39, pp. 361-374.

Fager, E. W. (1964). Marine Sediments: Effects of a Tube-building Polychaete. Science. v. 143, pp. 356-359.

Fauchald, K. and P. A. Jumars (1979). The Diet of Worms: A Study of Polychaete Feeding Guilds. Oceanogr. Mar. Biol. Ann. Rev. v. 17, pp. 193-284.

Folk, R. L. and W. C. Ward (1957). Brazos River Bar, a Study in the Significance of Grain Size Parameters. J. Sed. Pet. v. 27, pp. 3-26.

Freeland, G. L. and D. J. P. Swift (1978). Surficial Sediments. MESA New York Bight Atlas Monograph 10. New York Sea Grant Inst., Albany, N. Y. 93 pp.

Hamilton, E. L. (1970). Reflection Coefficients and Bottom Losses at Normal Incidence Computed from Pacific Sediment Properties. Geophys. v. 35, pp.995-1004.

Hamilton, E. L. (1971). Elastic Properties of Marine Sediments. J. Geophys. Res. v. 76, pp. 579-603.

Hamilton, E. L. (1972). Compressional Wave Attenuation in Marine Sediments. Geophys. v. 37, pp. 620-645.

Hamilton, E. L. (1980). Geoacoustic Modeling of the Sea Floor. J. Acoust. Soc. Am. v. 68, pp. 1313-1340.

Hamilton, E. L. and R. T. Bachman (1982). Sound Velocity and Related Properties of Marine Sediments. J. Acoust. Soc. Am. v. 72, pp. 1891-1904.

Horn, D. R., B. M. Horn and M. N. Delach (1968). Correlation Between Acoustic and Other Physical Properties in Deep-sea Cores. J. Geophys. Res. v. 73 pp. 1939-1957.

Mangum, C. P. (1964). Activity Pattern in Metabolism and Ecology of Polychaetes. Comparative Biochem. Physiol. v. 11, pp. 239-256.

Margalef, R. (1958). Information Theory in Ecology. Gen. Syst. v. 3, pp. 36-71.

McMaster, R. L. and L. E. Garrison (1967). A Submerged Holocence Shoreline Near Block Island, Rhode Island. Mar. Geol. v. 75, pp. 335-340.

Mills, E. L. (1967). The Biology of an Ampeliscid Amphipoda Crustacean Sibling Species Pair. J. Fish. Res. Bd. Can. v. 24, pp. 305-355.

Myers, A. C. (1977a). Sediment Processing in a Marine Subtidal Sandy Bottom Community: I. Physical Aspects. J. Mar. Res. v. 35, pp. 609-632.

Myers, A. C. (1977b). Sediment Processing in a Marine Subtidal Sandy Bottom Community: II. Biological Consequences. J. Mar. Res. v. 35, pp. 633-647.

Nafe, J. E. and C. L. Drake (1963). Physical Properties of Marine Sediments. In: M. N. Hill (ed.) The Sea, Vol. 3. Interscience, New York, N.Y. pp. 794-815.

Parker, G. H. (1927). Locomotion and Righting Movements in Echinoderms. Am. J. Psychol. v. 39.

Parker, G. H. and M. VanAlstyne (1932). Locomotor Organs of Echinarachnius parma. Biol. Bull. v. 62.

Pearce, J. B., D. J. Radosh, J. V. Caracciolo and F. W. Steimle (1981). Benthic Fauna. MESA New York Bight Atlas Monograph 14. New York Sea Grant Inst., Albany, N. Y. 79 pp.

Pielou, E. C. (1975). Ecological Diversity. John Wiley and Sons, New York, N.Y. 165 pp.

Rhoads, D. C. (1963). Rates of Sediment Reworking by Yoldia limatula in Buzzards Bay, Massachusetts, and Long Island Sound. J. Sed. Pet. v. 33, pp. 723-727.

Rhoads, D. C. (1967). Biogenic Reworking of Intertidal and Subtidal Sediments in Barnstable Harbor and Buzzards Bay, Massachusetts. J. Geol. vol. 75, pp. 461-476.

Rhoads, D. C. (1974). Organism-sediment Relations on the Muddy Sea-floor. Oceanogr. Mar. Biol. Ann. Rev. v. 12, pp. 263-300.

Richardson, M. D. and D. K. Young (1980). Geoacoustic Models and Bioturbation. Mar. Geol. v. 38, pp. 205-218.

Richardson, M. D., D. K. Young, K. B. Briggs (1983a). Effects of Hydrodynamic and Biological Processes on Sediment Geoacoustic Properties in Long Island Sound, U.S.A. Mar. Geol. v. 52, pp. 201-226.

Richardson, M. D., D. K. Young and R. I. Ray (1983b). Environmental Support for High Frequency Acoustic Measurements at NOSC Oceanographic Tower, 26 April-7 May 1982. NORDA Technical Note 219, 68 pp.

Roderick, W. I. (1982). Project WEAP Experimental and Analysis Plan: Preliminary Draft. NUSC unpublished document. New London, Conn. 20 pp.

Sanders, H. L. (1960). Benthic Studies in Buzzards Bay. III. The Structure of the Soft-bottom Community. Limnol. Oceanogr. pp. 138-153.

Schlee, J. (1973). Atlantic Continental Shelf and Slope of the United States--Sediment Texture of the Northeastern Part. Geological Survey Professional Paper. 529-L. 64 pp.

Stanic, S., M. D. Richardson, P. Fleischer (1983). Effects of Shallow-Water Environmental Processes on High Frequency Acoustic Scattering. NORDA unpublished document.

Swift, D. J. P., D. B. Duane and T. F. McKinney (1973). Ridge and Swale Topography of the Middle Atlantic Bight, North America: Secular Response to the Holocene Hydraulic Regime. Mar. Geol. v. 15, pp. 227-247.

Swift, D. J. P., J. W. Kofoed, F. P. Saulsburg and D. Sears (1972). Holocene Evolution of the Shelf Surface, Central and Southern Atlantic Shelf of North America. In: (D. J. P. Swift, D. B. Duane and O. H. Pilkey, eds.) Shelf Sediment Transport: Process and Pattern. Dowden, Hutchinson and Ross, Stroudsburg, Pa. pp. 499-574.

Wigley, R. L. and R. B. Theroux (1981). Atlantic Continental Shelf and Slope of the United States--Macrobenthic Invertebrate Fauna of the Middle Atlantic Bight Region--Faunal Composition and Quantitative Distribution. Geological Survey Professional Paper. 529-N, 198 pp.

Woodin, S. A. (1974). Polychaete Abundance in a Marine Soft-sediment Environment: The Importance of Biological Interactions. Ecol. Monogr. v. 44, pp. 171-187.

Woodin, S. A. (1976). Adult-larval Interactions in Dense Infaunal Assemblages: Patterns of Abundance. J. Mar. Res. v. 34, pp. 25-41.

Appendix A: Grain Size Distribution Data

Station 2-1

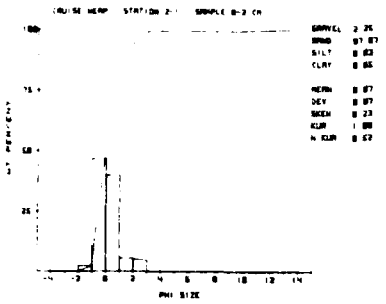

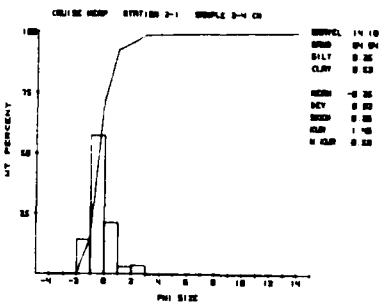

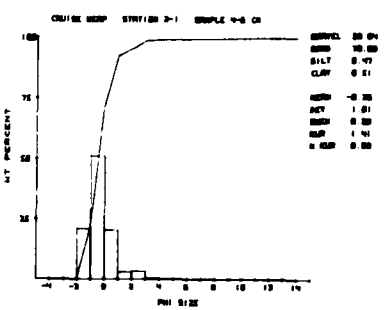

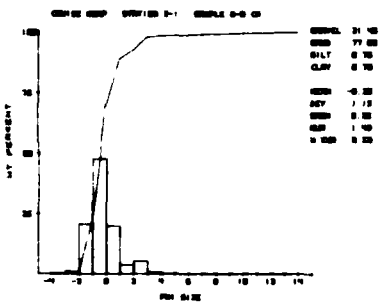

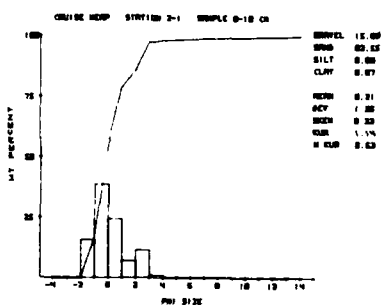

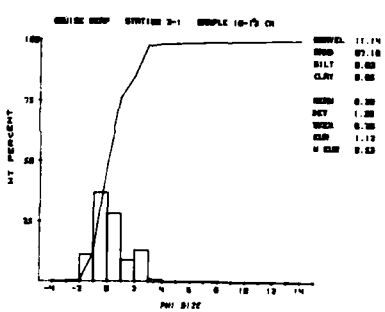

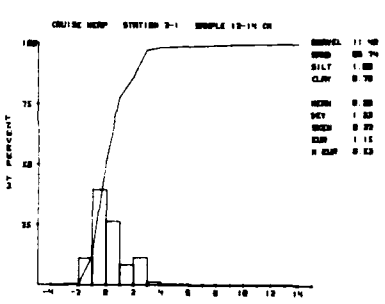

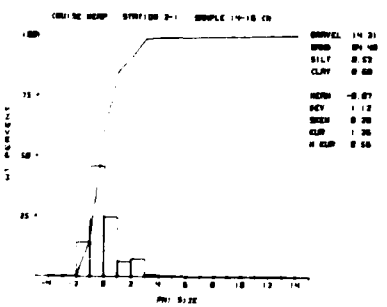

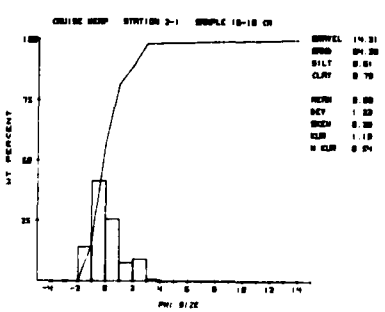

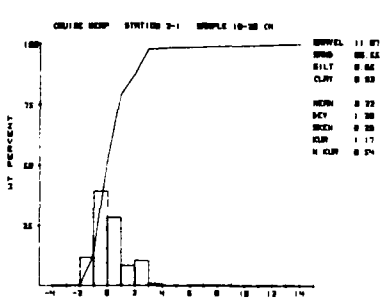

Station 2-2

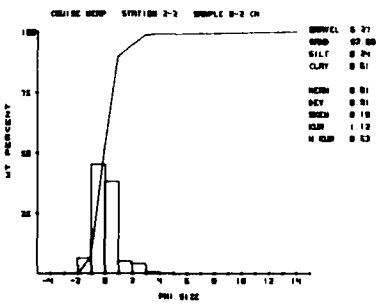

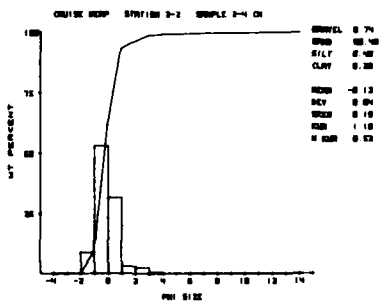

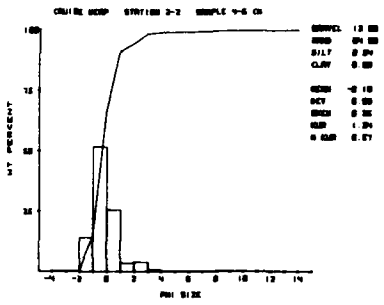

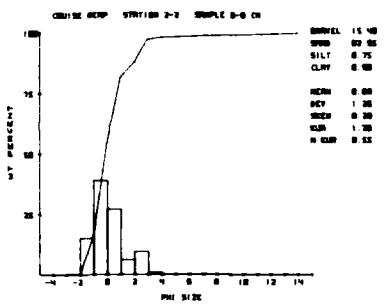

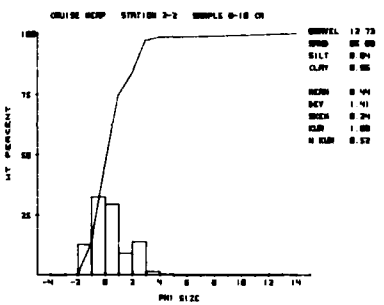

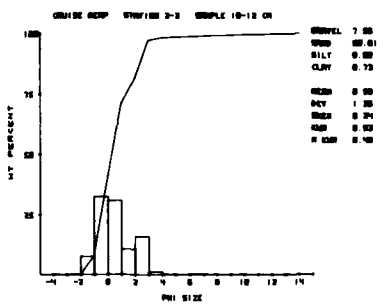

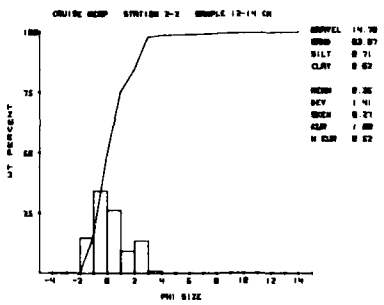

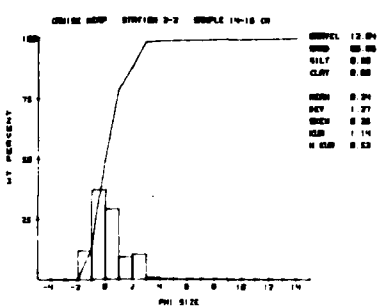

Station 3

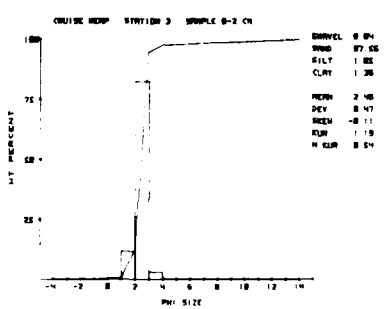

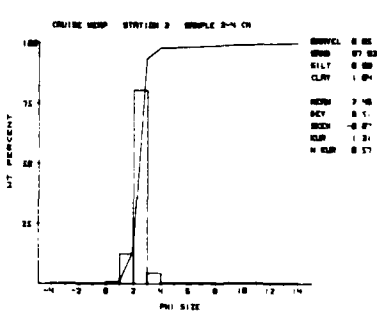

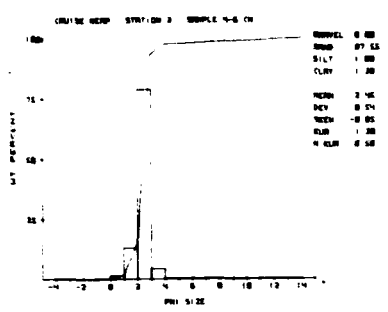

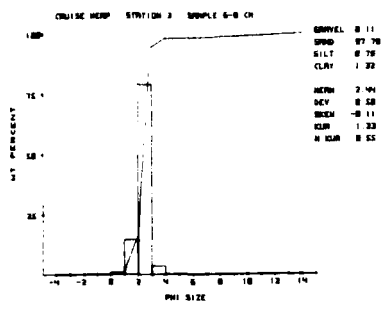

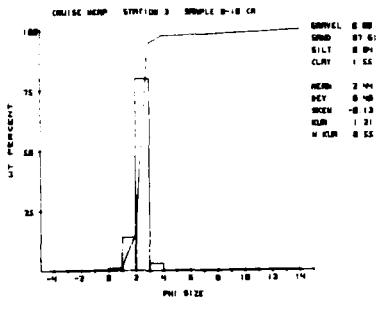

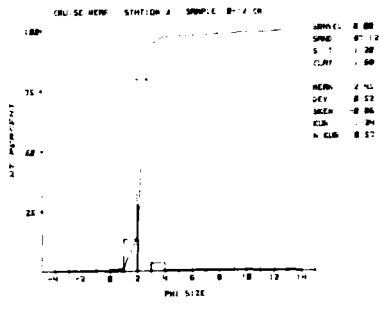

Station 4

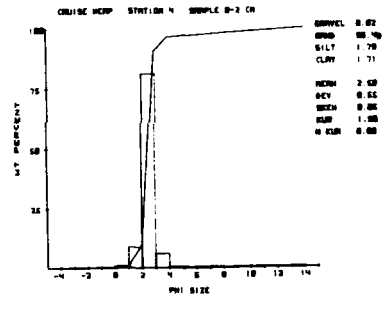

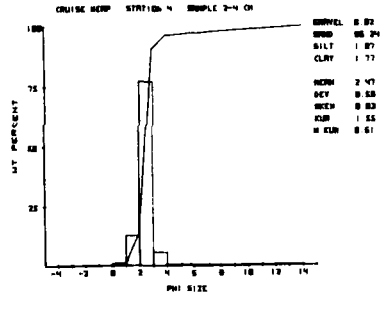

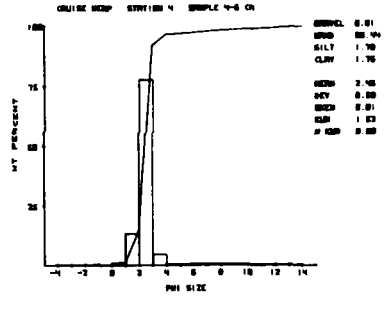

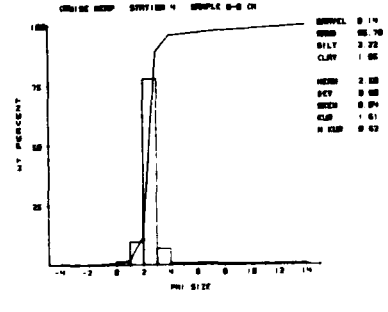

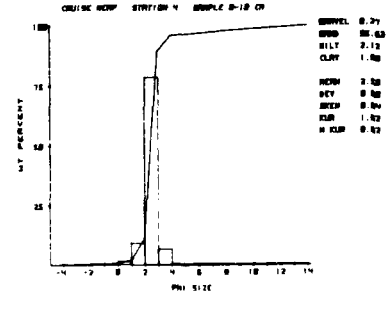

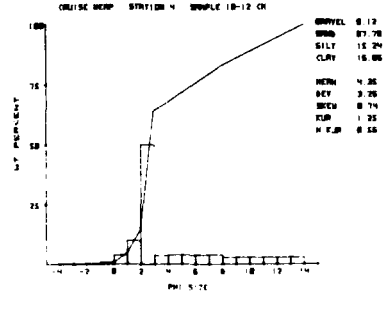

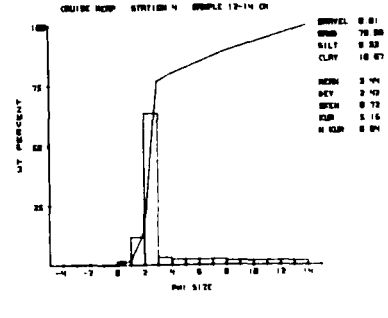

Station 5

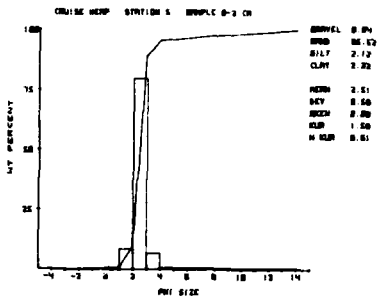

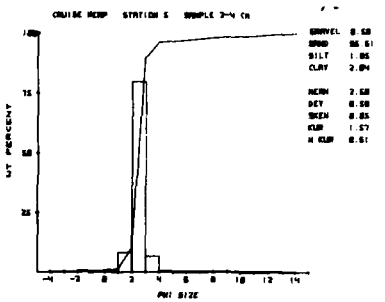

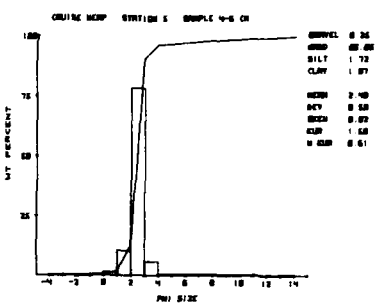

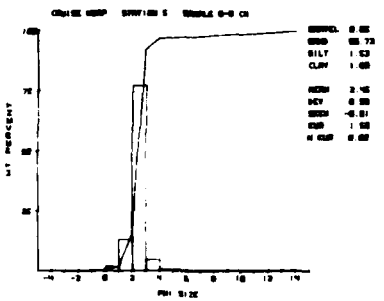

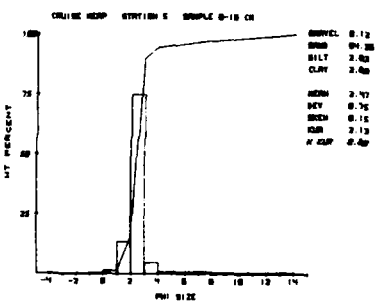

Station 6

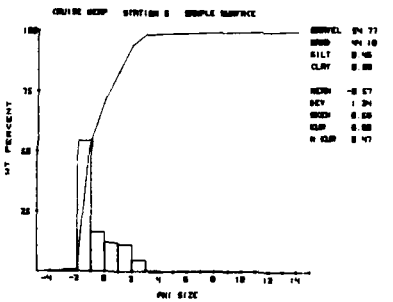

Station 7

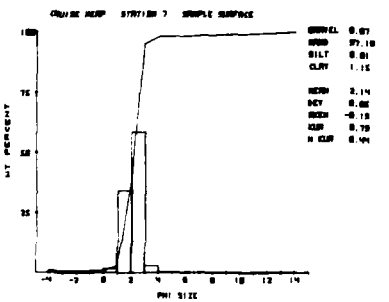

Station 8

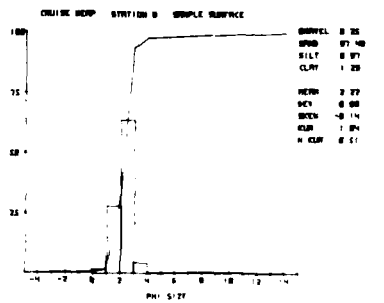

Station 9

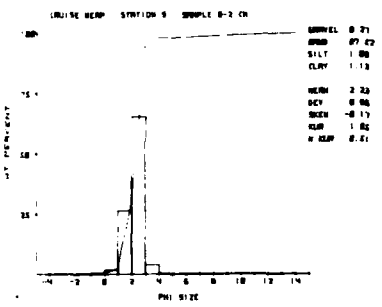

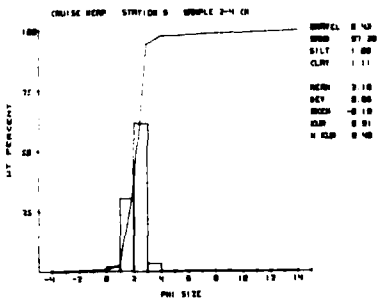

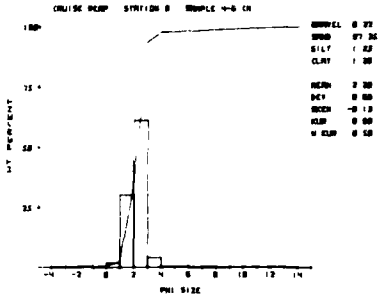

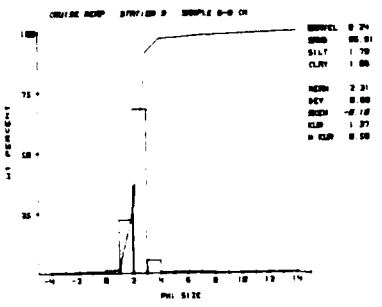

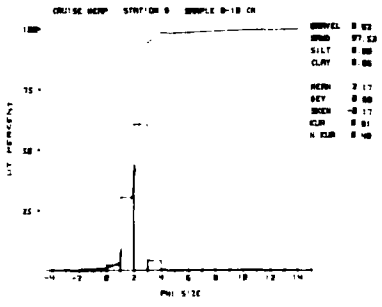

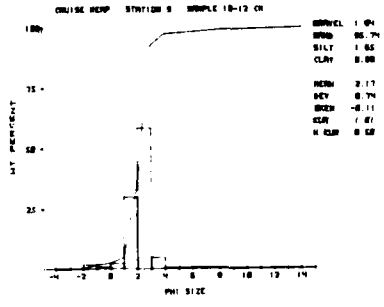

Station 10

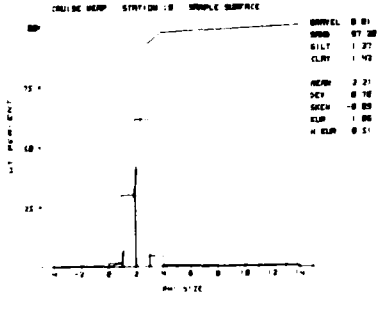

Station 11-1

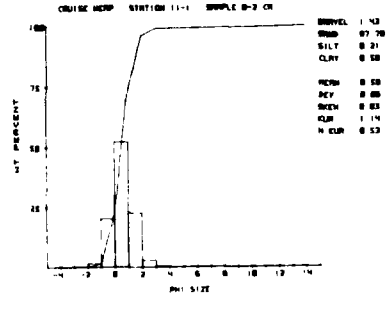

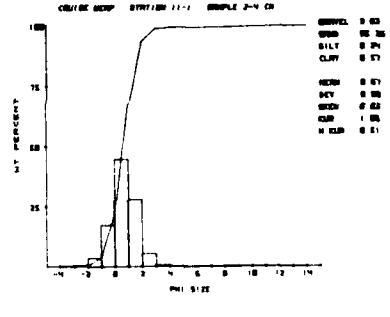

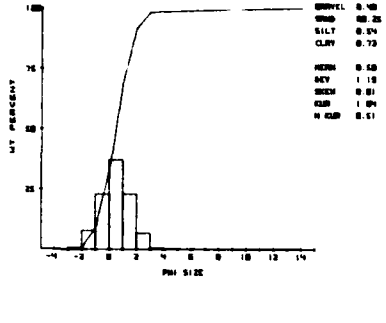

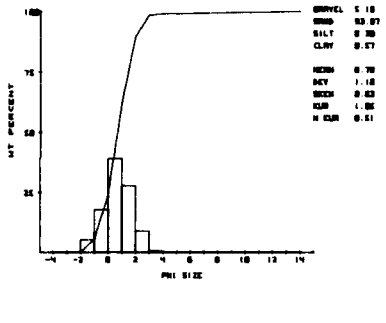

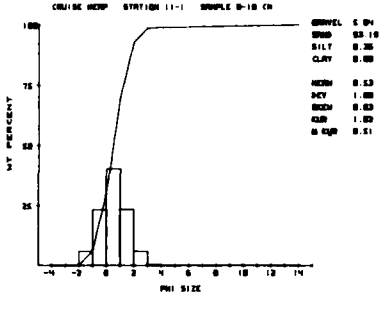

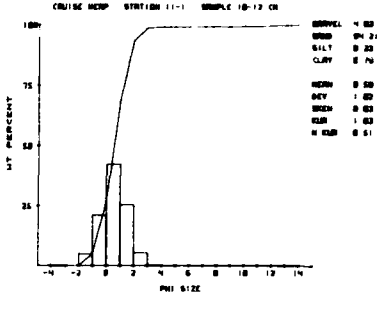

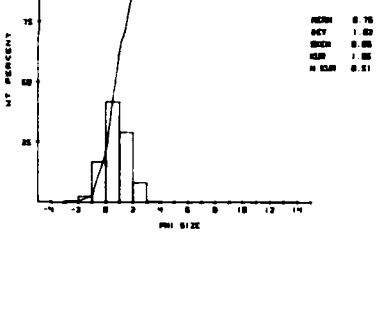

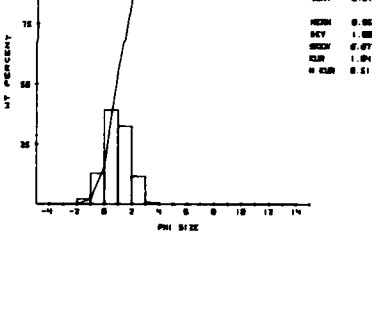

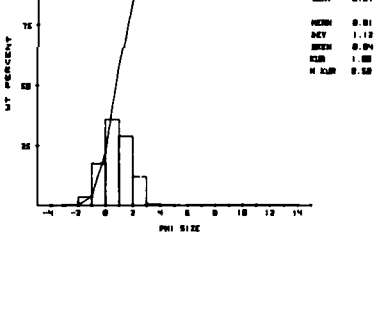

Station 12

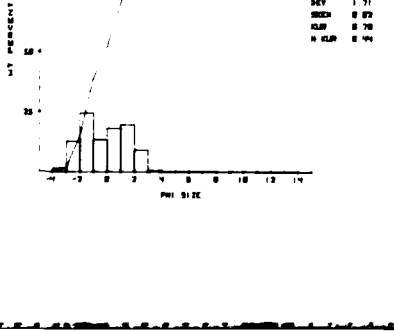

Station 13

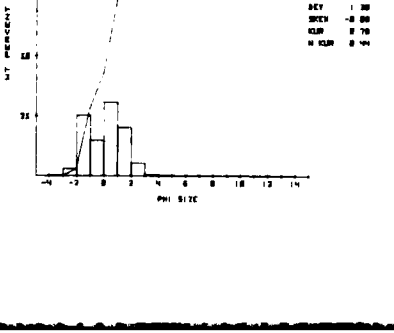

Station 14-1

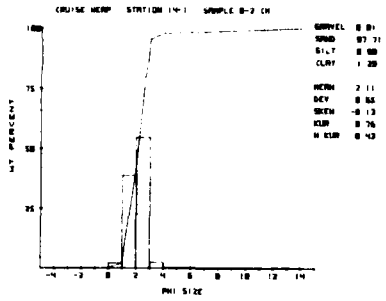

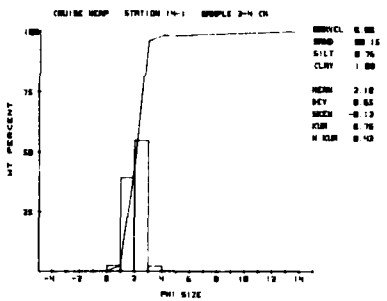

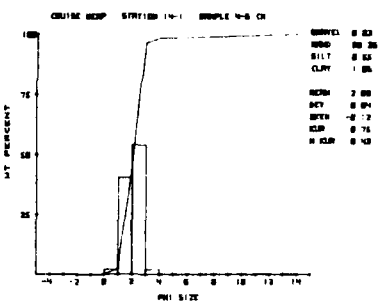

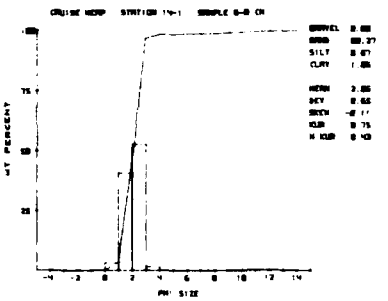

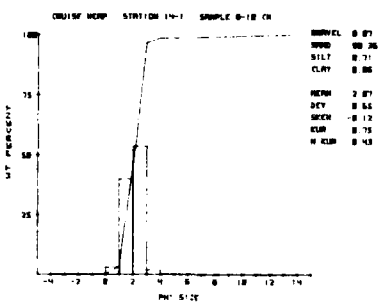

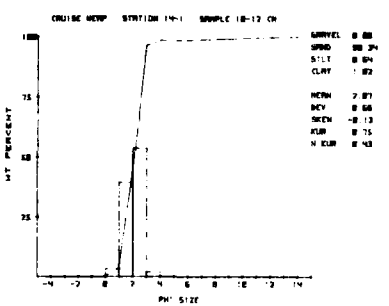

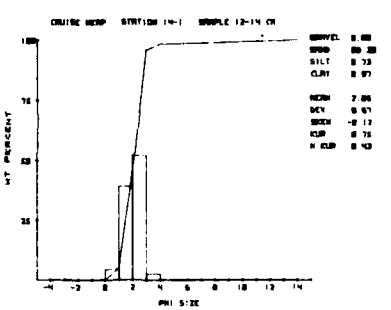

Station 14-2

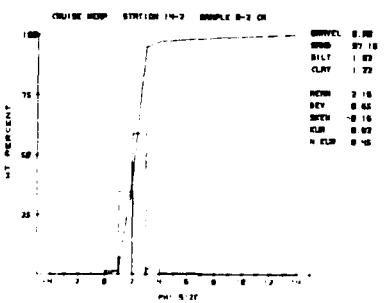

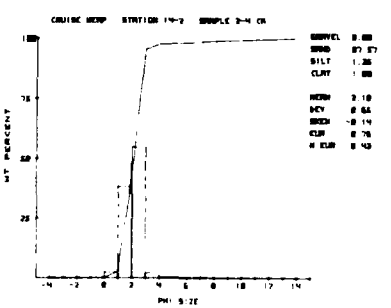

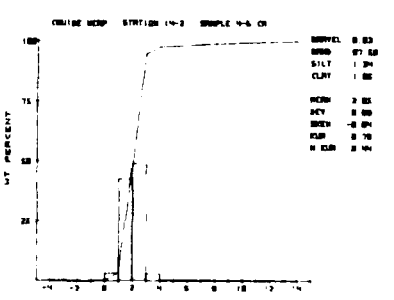

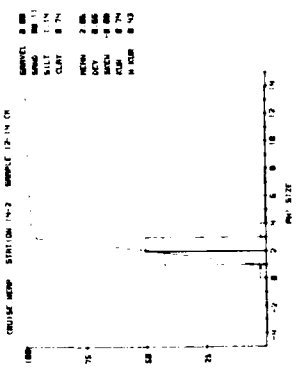

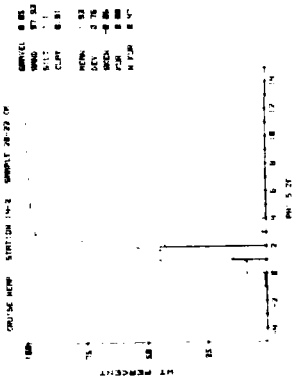

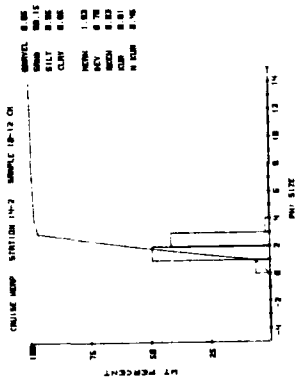

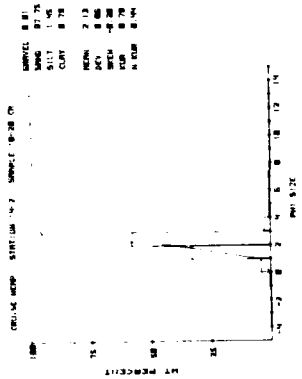

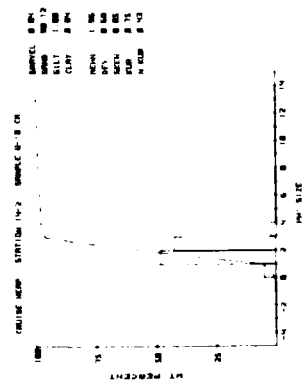

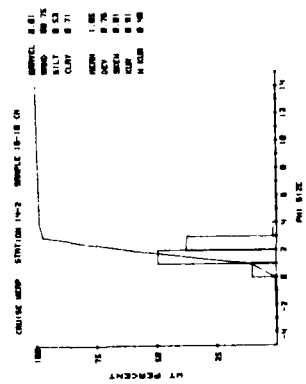

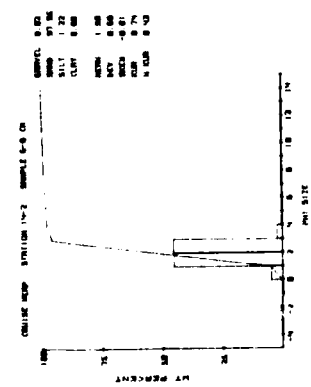

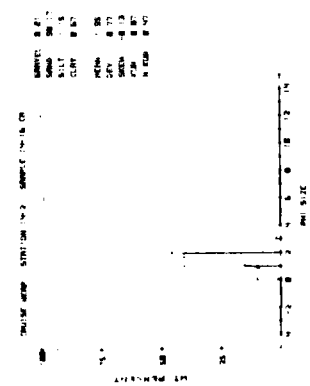

Distribution List

Department of the Navy
Asst Deputy Chief of Navy Materials
for Laboratory Management
Rm 1062 Crystal Plaza Bldg 5
Washington DC 20360

Department of the Navy
Asst Secretary of the Navy
(Research Engineering & System)
Washington DC 20350

Project Manager
ASW Systems Project (PM-4)
Department of the Navy
Washington DC 20360

Department of the Navy
Chief of Naval Material
Washington DC 20360

Department of the Navy
Chief of Naval Operations
ATTN: OP 951
Washington DC 20350

Department of the Navy
Chief of Naval Operations
ATTN: OP 952
Washington DC 20350

Department of the Navy
Chief of Naval Operations
ATTN: OP 987
Washington DC 20350

Director
Chief of Naval Research
ONR Code 420
Ocean Science & Technology Det
NSTL, MS 39529

Director
Defense Technical Info Cen
Cameron Station
Alexandria VA 22314

Commander
DW Taylor Naval Ship R&D Cen
Bethesda MD 20084

Commanding Officer
Fleet Numerical Ocean Cen
Monterey CA 93940

Director
Korean Ocean R&D Inst
ATTN: K. S. Song, Librarian
P. O. Box 17 Yang Jae
Seoul South Korea

Commander
Naval Air Development Center
Warminster PA 18974

Commander
Naval Air Systems Command
Headquarters
Washington DC 20361

Commanding Officer
Naval Coastal Systems Center
Panama City FL 32407

Commander
Naval Electronic Sys Com
Headquarters
Washington DC 20360

Commanding Officer
Naval Environmental Prediction
Research Facility
Monterey CA 93940

Commander
Naval Facilities Eng Command
Headquarters
200 Stovall St.
Alexandria VA 22332

Commanding Officer
Naval Ocean R & D Activity
ATTN: Codes 110/111
Code 125
Code 200
Code 300
Code 115
Code 500
NSTL MS 39529

Director
Liaison Office
Naval Ocean R & D Activity
800 N. Quincy Street
502 Ballston Tower #1
Arlington VA 22217

Commander
Naval Ocean Systems Center
San Diego CA 92152

Commanding Officer
Naval Oceanographic Office
NSTL MS 39522

Commander
Naval Oceanography Command
NSTL MS 39522

Superintendent
Naval Postgraduate School
Monterey CA 93940

Commanding Officer
Naval Research Laboratory
Washington DC 20375

Commander
Naval Sea System Command
Headquarters
Washington DC 20362

Commander
Naval Surface Weapons Center
Dahlgren VA 22448

Commanding Officer
Naval Underwater Systems Center
ATTN: New London Lab
Newport RI 02840

Director
New Zealand Oceano Inst
ATTN: Library
P. O. Box 12-346
WELLINGTON N., NEW ZEALAND

Director
Office of Naval Research
Ocean Science & Technology Div
NSTL MS 39529

Department of the Navy
Office of Naval Research
ATTN: Code 102
800 N. Quincy St.
Arlington VA 22217

Commanding Officer
ONR Branch Office
536 S Clark Street
Chicago IL 60605

Commanding Officer
ONR Branch Office LONDON
Box 39
FPO New York 09510

Commanding Officer
ONR Western Regional Ofs
1030 E. Green Street
Pasadena CA 91106

President
Texas A&M
ATTN: Dept of Ocean Working Collection
College Station TX 77843

Director
University of California
Scripps Institute of Oceanography
P. O. Box 6049
San Diego Ca 92106

Director
Woods Hole Oceanographic Inst
Woods Hole MA 02543

UNCLASSIFIED

SECURITY CLASSIFICATION OF THIS PAGE *(When Data Entered)*

REPORT DOCUMENTATION PAGE		READ INSTRUCTIONS BEFORE COMPLETING FORM
1. REPORT NUMBER NORDA Report 40	2. GOVT ACCESSION NO. AD-A139 800	3. RECIPIENT'S CATALOG NUMBER
4. TITLE *(and Subtitle)* Environmental Support for Project WEAP East of Montauk Point, New York 7-28 May 1982		5. TYPE OF REPORT & PERIOD COVERED Final 6. PERFORMING ORG. REPORT NUMBER
7. AUTHOR(s) Michael D. Richardson John H. Teitjen * Richard I. Ray		8. CONTRACT OR GRANT NUMBER(s)
9. PERFORMING ORGANIZATION NAME AND ADDRESS Naval Ocean Research and Development Activity NSTL, Mississippi 39529		10. PROGRAM ELEMENT, PROJECT, TASK AREA & WORK UNIT NUMBERS 62759N
11. CONTROLLING OFFICE NAME AND ADDRESS Naval Ocean Research and Development Activity NSTL, Mississippi 39529		12. REPORT DATE October 1983 13. NUMBER OF PAGES 52
14. MONITORING AGENCY NAME & ADDRESS*(if different from Controlling Office)*		15. SECURITY CLASS. *(of this report)* UNCLASSIFIED 15a. DECLASSIFICATION/DOWNGRADING SCHEDULE

16. DISTRIBUTION STATEMENT *(of this Report)*

Approved for Public Release. Distribution Unlimited.

17. DISTRIBUTION STATEMENT *(of the abstract entered in Block 20, if different from Report)*

18. SUPPLEMENTARY NOTES

* City College of New York
Deppartment of Biology
New York, N.Y. 10031

19. KEY WORDS *(Continue on reverse side if necessary and identify by block number)*

sediment geoacoustic properties
bioturbation
high frequency acoustic scattering
environmental acoustic support

20. ABSTRACT *(Continue on reverse side if necessary and identify by block number)*

This report covers environmental support for project WEAP (Weapons Environmental Acoustic Program), a joint Naval Underwater Systems Center (NUSC), Naval Ocean Research and Development Activity (NORDA) high frequency acoustic experiment, conducted 25 km east of Montauk Point, Long Island, New York. The objective of Project WEAP was to provide the high resolution acoustic and environmental data required for new concepts in weapon system design.

(continued)

DD FORM 1 JAN 73 1473 EDITION OF 1 NOV 65 IS OBSOLETE
S/N 0102-LF-014-6601

UNCLASSIFIED

SECURITY CLASSIFICATION OF THIS PAGE *(When Data Entered)*

(continued from Block 20)

The acoustic experiment was sited at the southern terminus of a drowned barrier spit in 35 m of water. Sediment and faunal samples were collected remotely with a 0.025 m^2 box core. Diver (scuba) collected sediment cores were obtained to measure sediment geoacoustic properties.

Two sediment types (fine sand and coarse sand) were evident from the laboratory analysis of sediment grain size. Fine sand sediments had lower values of compressional wave velocity, impedance, and bulk density; lower reflection coefficients and higher bottom loss and attenuation values than coarse sand sediments.

Geoacoustic Property	Sediment Type	
	Fine Sand	Coarse Sand
Mean Grain Size (Ø)	2.07	0.00
Porosity (%)	36.5	----
Sediment Density (g/cm^3)	2.05	2.37
Compressional Wave Velocity (m/sec) @ 6°C, 32.4 ppt, 36 m	1677	1728
Attenuation (k)	0.22	0.17
Sediment Impedance ($g/cm^2 sec$ 10^5) @ 6°C, 32.4 ppt, 36 m	3.41	4.1
Rayleigh Reflection Coefficient	0.39	0.46
Bottom Loss (dB) @ normal incidence	8.3	6.7

Measured compressional wave velocity values were 3 to 5 percent lower than the values derived from empirical predictor equations for fine sand sediments, while attenuation values were one-half predicted values. We estimate that predicted compressional wave velocity for coarse sand was 8 percent higher than actual values. We, therefore, calculated sediment geoacoustic properties for coarse sand sediments based on compressional wave velocity of 1728 m/sec instead of the empirically predicted 1878 m/sec. This yielded lower than predicted (from mean grain size) sediment impedance and reflection coefficients and higher bottom loss. Estimated attenuation values were also lower than those empirically predicted.

The within core and within station variability of sediment geoacoustic properties was low, partially a result of sediment mixing by benthic invertebrates. The areal (between station) variability in sediment geoacoustic properties was high because present hydrodynamic and historical geological processes created a two sediment system: a light-colored, well-sorted, fine sand discontinously covered a reddish, coarse, granular sediment.

The fine sand was similar to most sediments found on the middle Atlantic Sand Plain. This sediment was derived from weathering products transported from adjacent land during previous glacial regressions. The reddish coarse

(continued from Block 20)

sand was a lag deposit formed from the erosion of the drowned barrier spit. The fine sand was in dynamic equilibrium with severe storms which occur in this area while the coarse sand was in equilibrium with rarer, very severe storms. The areal distribution of these sediment types was not predictable from historical data and probably changes with season and severe storm events. Side scan sonar imagery techniques are required to delineate the distribution of both sediment types. Had the experiment been sited 10 m deeper sediment geoacoustic properties and microtopography could have been more precisely predicted, because of less heterogenity in sediments.

The distribution of faunal assemblages paralleled the distribution of sediment types. The fine sand substrate (Stations 3, 4, 5, 7, 8, 9, and 10) was dominated by tube-building ampeliscid amphipods, free-burrowing haustoriid amphipods, and the sand dollar, Echinarachnius parma. Amphipods contributed 55 percent of the faunal density at these stations while sand dollars accounted for 79 percent of the biomass. The coarse sand substrate (Stations 6, 11, 12, and 13) was dominanted by the errant polychaetes Drilonereis magna, Drilonereis longa, Goniada maculata and Glycera capitata. Also abundant was the tube-dwelling polychaete Clymenella torquata.

Bioturbation by the sand dollar, Echinarachinius parma, mixed the upper few centimeters of sediment, changing sediment geoacoustic properties and modifying and distroying microtopography. E. parma probably contributes to surface forward and backscatter at 40 and 80 kHz where their calcareous bodies act as point surface scatterers, and at all frequencies where sand dollars overlap. The sediment microtopography created by E. parma probably contributes to resonance scattering of all frequencies used in Project WEAP (5 to 80 kHz).

It is estimated that, the tube dwelling polychaete Clymenella torquata turns over the upper 20 cm of sediment at one station in 0.42 yr. This activity may create considerable microtopography and sediment volume heterogeneity in geoacoustic properties, which probably contributes to resonance and volume scattering at the coarse sand stations.

Recommendations for future shallow-water acoustic experiments are given. Collection of in-situ environmental data is suggested. The use of extensive presite surveys is strongly urged in order to site the experiment in a homogeneous area or at least in an area where heterogeneities can be predicted and mapped. Detailed methodologies and philosophies for environmental sampling are given. These approaches should yield the physical and empirical submodels required to extrapolate acoustic bottom reverberation prediction beyond the measured data.

END

FILMED

5-84

DTIC